VIA MEDICA

ROZPRAWA HABILITACYJNA

Journal of Transfusion Medicine
2009, tom 2, nr 1, 41–72

ISSN 1689–6017

Pathogenetic mechanisms and therapeutic targets in diffuse large B-cell lymphomas characterized by constitutive tonic B-cell receptor activity and BCL6 transcriptional program: from DNA microarrays to rational therapy

Mechanizmy patogenetyczne i cele terapeutyczne w chłoniaku rozlanym z dużych komórek B zależne od konstytutywnej aktywności tonicznej receptora B-komórkowego i programu transkrypcyjnego BCL6: od mikromacierzy DNA do racjonalnego leczenia

Przemysław Juszczyński

Dana Faber Cancer Institute, Harvard Medical School

Table of Contents

Adres do korespondencji: Przemysław Juszczyński, MD, PhD, Dana Farber Cancer Institute, Harvard Medical School Department of Medical Oncology, 44 Binney Street, Mayer Building, Room M515, Boston, MA 02115, tel.: (617) 632 4749 faks: (617) 632 4734, e-mail: przemyslaw_juszczynski@dfci.harvard.edu

Streszczenie

Wielkokomórkowe chłoniaki rozlane B-komórkowe (DLBCL, diffuse large B-cell lymphoma*) są najczęstszymi nowotworami układu chłonnego u ludzi dorosłych, a zarazem niezwykle heterogenną grupą chorób. Ich molekularną substrukturę odzwierciedlają w znacznym stopniu biologiczne uwarunkowania, scharakteryzowane uprzednio na podstawie globalnego profilu ekspresji genów i algorytmu* consensus clustering *w dwóch niezależnych grupach chorych. Badania te wykazały, że w obrębie chłoniaków DLBCL można wyróżnić trzy podtypy o odmiennej genetycznej charakterystyce. Profil ekspresji najliczniejszej ze zidentyfikowanych grup, nazwanej „BCR" (*B-cell receptor signaling*), charakteryzowała nadekspresja genów kodujących białka receptora B-komórkowego i kaskady transdukcji sygnału z tego receptora, w tym SYK (*Spleen Tyrosine Kinase*) oraz niektóre B-komórkowe czyniki transkrypcyjne, w tym BCL6. W grupie "BCR" obserwowano również częstsze niż w innych podtypach translokacje regionu 3q obejmujące locus BCL6. Obserwacje te sugerowały, że wzrost i proliferacja komórek tego molekularnego podtypu DLBCL może zależeć od ścieżek sygnałowych zależnych od receptora BCR i/lub od programu transkrypcyjnego BCL6. W celu zbadania tej hipotezy, przeprowadzono badania oceniające rolę tonicznego sygnału zależnego od kinazy SYK i konsekwencji inhibicji transdukcji tego sygnału* in vitro*, mechanizmy kontrolujące aktywność kinazy SYK, mechanizmy transkrypcyjne czynnika transkrypcyjnego BCL6 i konsekwencje wyłączenia funkcji BCL6* in vitro *oraz interakcję pomiędzy funkcją czynnika transkrypcyjnego BCL6 i aktywnością receptora BCR w chłoniakach o molekularnej charakterystyce „BCR".*

*W przeprowadzonych badaniach wykazano, że zarówno linie komórkowe o charakterystyce molekularnej odpowiadającej chłoniakom typu „BCR", jak i pierwotne izolowane komórki nowotworowe pobrane od części chorych, wykazują konstytutywną toniczną aktywność kinazy SYK i jej bezpośredniego substratu, białka adaptorowego BLNK (*B-cell linker protein*). Zastosowanie wysokospecyficznego, ATP-kompetycyjnego inhibitora R406* in vitro *prowadziło do zahamowania tonicznej i aktywowanej ligandem aktywności receptora BCR (mierzonej jako fosforylacja BLNK84) i prowadziło do apoptozy badanych komórek. Badania te wskazują, że SYK-zależny toniczny sygnał receptora BCR jest ważnym czynnikiem warunkującym proliferację komórek chłoniakowych o molekularnej charakterystyce „BCR" i może być terapeutycznym celem dla małocząsteczkowego inhibitora SYK. Wykazano ponadto, że komórki wrażliwe na działanie tego inhibitora można zidentyfikować na podstawie ich globalnego profilu ekspresji genów.*

*Kluczowa rola SYK w transdukcji i amplifikacji sygnału z receptora BCR sugerowała, że aktywność tej kinazy pozostaje pod ścisłą fizjologiczną kontrolą. W drugiej części badań wykazano, że kinaza ta jest substratem dla tkankowo-swoistej izoformy fosfatazy PTPROt (*Protein Tyrosine Phosphatase, Receptor–type O, truncated*). Wymuszona ekspresja PTPROt prowadziła do zahamowania fosforylacji SYK indukowanej ligandem i dystalnej blokady w transdukcji sygnału do kinaz ERK1/2. Nadekspresja PTPROt prowadziła również do zahamowania proliferacji komórek, a w konsekwencji do ich apoptozy. Apoptotyczną śmierć komórek*

wskutek nadekspresji PTPROt obserwowano również przy braku aktywacji receptora BCR, co sugeruje, że fosfataza ta reguluje także toniczną aktywność SYK.

*Drugą podstawową charakterystyką chłoniaków DLBCL typu „BCR" jest nadekspresja czynnika transkrypcyjnego BCL6 i częstsze translokacje dotyczące tego onkogenu. Obserwacje te sugerowały, że ekspresja BCL6 może być dodatkowym czynnikiem warunkującym wzrost w tym podtypie molekularnym DLBCL. Chłoniaki DLBCL zależne od szlaków molekularnych regulowanych przez BCL6 powinny wykazywać skoordynowany profil ekspresji genów kontrolowanych przez BCL6, odrębny od profilu chłoniaków niezależnych od BCL6. W celu zbadania tej hipotezy, przeprowadzono genomową analizę regionów promotorowych regulowanych przez BCL6. Wykazano, że geny kontrolowane przez BCL6 były istotnie częściej reprezentowane w grupie „BCR". W badaniach przeprowadzonych na liniach komórkowych, proapoptotyczny efekt inhibicji funkcji BCL6 peptydem BPI (*BCL6-peptide inhibitor*) obserwowano wyłącznie w liniach typu „BCR".*

Unikalna wrażliwość linii komórkowych typu „BCR" na inhibicję BCL6 sugerowała istnienie nieznanego dotychczas związku między działaniem tego czynnika transkrypcyjnego a sygnałem zależnym od receptora BCR. Celem zbadania postulowanego związku, przeanalizowano wpływ czynnika transkrypcyjnego BCL6 na poziom transkrypcji genów kodujących białka biorące udział w proksymalnych etapach transdukcji sygnału z BCR. W izolowanych, wysoko oczyszczonych frakcjach prawidłowych limfocytów, w tym naiwnych, germinalnych i komórkach pamięci oraz w dwóch grupach pacjentów z DLBCL, ekspresja transkryptu BCL6 pozostawała w odwrotnej korelacji z ekspresją transkryptu PTPROt. W dalszych badaniach funkcjonalnych wykazano, że BCL6 jest represorem transkrypcji genu PTPROt i bezpośrednio wiąże się z jego regionem promotorowym. Wyłączenie funkcji BCL6 poprzez mechanizm interferencji RNA powodowało nadekspresję PTPROt, defosforylację SYK oraz zahamowanie transdukcji sygnału z receptora BCR tylko w liniach komórkowych typu „BCR". BCL6 kontrolował promotor PTPROt również w prawidłowych izolowanych germinalnych limfocytach B, wskazując, że BCL6 jest fizjologicznym regulatorem przekazywania sygnału z BCR. Przeprowadzone badania identyfikują dotychczas nieznaną funkcję BCL6 w regulacji aktywności kompleksu receptora BCR oraz wskazują na istotny mechanizm wrażliwości na inhibicję BCL6, zależny od zahamowania aktywności kinazy SYK. Badania te sugerują również, że skojarzone zahamowanie szlaków sygnałowych zależnych od BCL6 i receptora B-komórkowego może mieć charakter synergistyczny u chorych z chłoniakami DLBCL o charakterystyce molekularnej "BCR".

Słowa kluczowe: Wielkokomórkowe chłoniaki rozlane B-komórkowe, Mikromacierze DNA, Profil ekspresji genów, Receptor B-komórkowy, SYK, PTPROt, BCL6, Terapia celowana

Summary

Diffuse large B-cell lymphomas (DLBCL) are the most common lymphoid malignancy in adults and an extremely heterogeneous group of disorders. To delineate functionally relevant DLBCL subsets, consensus clustering methods were previously applied to the transcriptional profiles of two large independent series of primary DLBCL to identify the dominant substructure a priori. *The obtained consensus clusters were highly reproducible and included a group of DLBCL, termed B-cell receptor ("BCR") that was characterized by increased expression of components of the BCR signaling cascade including SYK (Spleen Tyrosine Kinase) and certain B-cell specific transcription factors such as BCL6; these DLBCL also exhibit more frequent translocations of the BCL6 locus. These observations suggested that the "BCR" molecular category of DLBCL might be reliant on either, or both, BCR signaling and BCL6 transcriptional program. To test this hypothesis, the studies were undertaken to specifically investigate the role of tonic SYK-dependent signaling in "BCR"-type DLBCL and the biologi-*

cal consequences of the pathway inhibition in vitro*, mechanisms controlling SYK activity, role of transcriptional program controlled by BCL6 and the biological consequences of its inhibition* in vitro *and relationship between BCL6 mediated repression and SYK-dependent signaling in "BCR"-type DLBCL.*

These studies demonstrated that inhibition of the BCR signaling pathway with an ATP-competitive inhibitor of SYK, R406, induced apoptosis of the majority of examined DLBCL cell lines and primary DLBCL in vitro*. R406-sensitive DLBCL cell lines and primary tumors exhibited tonic activity of SYK and its direct substrate, B-cell linker protein (BLNK). In these R406-sensitive lines and primary tumors, R406 specifically inhibited both tonic and ligand-induced BCR signaling (SYK-dependent phosphorylation of BLNK). Therefore, SYK-dependent tonic BCR signaling is an important and potentially targetable survival pathway in some, but not all, DLBCL. In addition, R406-sensitive DLBCL can be identified by their transcriptional profiles.*

Consistent with critical role of SYK in modulating BCR signaling, its activity remains under tight control. SYK is a major substrate of a tissue-specific and developmentally regulated PTP, PTP receptor–type O truncated (PTPROt). The overexpression of PTPROt inhibited BCR--triggered SYK tyrosyl phosphorylation and downstream signaling events, including extracellular signal–regulated kinase (ERK1/2) activation. PTPROt overexpression also inhibited lymphoma cell proliferation and induced apoptosis in the absence of BCR cross-linking, suggesting that the phosphatase modulates tonic BCR signaling.

"BCR" tumors also exhibit more abundant BCL6 expression and more frequent BCL6 translocations, suggesting that these tumors likely rely on BCL6 transcriptional program. It could be predicted therefore that DLBCL dependent upon BCL6-regulated pathways would exhibit coordinate repression of BCL6 target genes. For this reason, genomic array ChIP-on-chip was utilized to identify the cohort of direct BCL6 target genes. In primary DLBCL classified on the basis of gene expression profiles, these BCL6 target genes were differentially regulated in "BCR" tumors. In a panel of DLBCL cell lines analyzed by expression arrays and classified according to their gene expression profiles, only "BCR" tumors were highly sensitive to the BCL6 peptide inhibitor (BPI). These studies identify a discrete subset of DLBCL that are reliant upon BCL6 signaling and uniquely sensitive to BCL6 inhibitors.

Since the same transcriptionally defined subset of DLBCL relies upon SYK-dependent BCR signaling and exhibits coordinate BCL6-mediated transcriptional repression, the relationship between these two processes was subsequently explored. In transcriptionally profiled normal B-cell subsets (naïve, germinal center [GC], and memory B cells) and in primary DLBCL, there were reciprocal patterns of expression of BCL6 and the SYK tyrosine phosphatase, PTPROt. BCL6 repressed PTPROt transcription via a direct interaction with functional BCL6 binding sites in PTPROt promoter. Enforced expression of BCL6 in normal naïve B cells and RNAi-mediated depletion of BCL6 in GC B-cells directly modulated PTPROt expression. In "BCR"-type DLBCL, BCL6 depletion increased PTPROt expression and decreased phosphorylation of SYK and the downstream adaptor protein, BLNK, demonstrating that BCL6 augments BCR signaling. Since BCL6 and SYK are both promising therapeutic targets in many DLBCL, combined inhibition of these functionally related pathways warrants further study.

Key words: Diffuse large B-cell lymphomas, Microarray gene expression profiling, B-cell receptor, SYK, PTPROt, BCL6 transcriptional program, Targeted therapy

List of abbreviations

BCR:	B-cell receptor
"BCR":	"B-cell Receptor" Consensus Cluster
BPI:	BCL6 peptide inhibitor
ChIP:	chromatin immunoprecipitation
CR:	complete response
C_T:	threshold cycle
CLL/SLL:	chronic lymphocytic leukemia/small lymphocytic lymphoma
DLBCL:	diffuse large B-cell lymphoma
ERK :	extracellular signal–regulated kinase
ES:	enrichment score
FDR:	false discovery rate
FL:	follicular lymphoma
GC:	germinal center
GO:	Gene Ontology
GSEA:	gene-set enrichment analysis
"HR":	"Host Response" Consensus Cluster
IC50:	inhibitory concentration for 50% cells
Ig:	immunoglobulin
IPI:	International Prognostic Index
ITAM:	immunoreceptor tyrosine-based activation motif
MALT:	mucosa-associated lymphoid tissue
MCL:	mantle cell lymphoma
PI :	propidium iodide
PTK:	protein tyrosine kinase
PTP:	protein tyrosine phosphatase
PTPROt :	protein tyrosine phosphatase receptor type O, truncated
MTT:	3-(4,5-dimethylthiazol-2-yl)-2,5-diphenyltetrazolium bromide assay
NHL:	non-Hodgkin lymphoma
"OxP" :	"Oxydative Phosphorylation" Consensus Cluster
PR:	partial response
QChip:	quantitative single-locus chromatin immunoprecipitation
SD:	standard deviation
SHM:	somatic hypermutation
SNR:	signal-to-noise ratio
SYK:	spleen tyrosine kinase
TSS:	transcription start site

Introduction

Heterogeneity of DLBCL

Diffuse large B-cell lymphomas (DLBCL) are the most common lymphoid malignancies in adults [1]. DLBCL are thought to arise from normal antigen-exposed B cells that have migrated to or through germinal centers (GC) of lymph nodes or secondary lymphoid organs [2]. Like normal GC B cells and their progeny, DLBCL have somatic hypermutations (SHM) of immunoglobulin receptor variable (v) region genes [3, 4]. Physiologically, SHM occurs during GC B-lymphocyte development and generates antibody diversity and increases antigen affinity. As this process involves generation of transient double strand DNA brakes, SHM also facilitates chromosomal translocations and mutagenesis that deregulate expression of certain oncogenes, such as BCL6, BCL2, or cMYC [1, 3, 5, 6]. A subset of DLBCL also exhibits aberrant SHM of genes that are not targeted by this editing process in normal GC B cells [7]. Finally, a significant percentage of DLBCL lack known genetic abnormalities.

The pathogenetic heterogeneity of this disease is reflected by the clinical variability in the disease course. Although approximately 50–55% of DLBCL patients can be cured with modern therapy, the remaining patients succumb to their disease [1]. Clinical prognostic models such as the International Prognostic Index (IPI) can be used to robustly identify patients who are less likely to be cured with standard chemotherapy [8]. Although such models were proven extremely useful clinically, they provide solely descriptive risk assessment and do not provide specific insights regarding tumor cell biology, alternative more effective treatment strategies or novel therapeutic targets.

Molecular substructure of DLBCL

Striking clinical and genetic heterogeneity suggest additional substructure within DLBCL. To unveil this molecular substructure in an unbiased way, a genome-wide genetic profiling and multiple clustering methods (hierarchical clustering, probabilistic clustering, and self-organizing maps) have been previously applied to 176 newly identified DLBCL patients [9]. Using an approach that assessed an agreement between the 3 clustering algorithms and selected the most stable numbers of clusters with each algorithm, 3 biologically robust clusters were defined that were independent of prior distinctions, such as Cell of Origin (COO) [9–11]. Within each cluster, overexpressed genes and pathways were identified and analyzed to indicate the most likely biological background of the subset and provide clues to lymphomagenesis. The first cluster, termed "Oxidative Phosphorylation" (OxP), showed increased expression of genes involved in mitochondrial function, electron transport, regulation of apoptosis, and proteosomal degradation [9]. Genetically, these tumors were more likely than others to harbor the t(14;18) involving BCL2 [9, 12]. The signature of the second cluster, termed "Host

Response" (HR) was largely determined by the host inflammatory response, rather than tumor cells themselves. In HR tumors, overexpressed genes included those involved in T-cell receptor signaling, CD2, T-cell and natural killer (NK) cell activation, monocyte/macrophage activators, complement pathway proteins, cytokine receptors, tumor necrosis factor (TNF)–related proteins, and adhesion molecules [9]. The third cluster, accounting for more than 50% of tumors, was characterized primarily by increased expression of components of the BCR signaling cascade and certain B-cell–specific transcription factors, such as BCL6. Of note, these tumors also had more frequent standalone BCL6 translocations, suggesting that these tumors likely rely on the BCR signaling cascade and BCL6 transcriptional program and that these pathways could represent novel rational treatment targets [12].

Tonic BCR signaling in normal B-cell development and in DLBCL

Emerging data highlight the important role of B-cell receptor (BCR)-mediated survival signals during normal B-cell development and in certain B-cell lymphomas. BCR engagement induces receptor oligomerization and phosphorylation of Iga and b immunoreceptor tyrosine-based activation motifs (ITAMs) by SRC family kinases [13–15]. ITAM phosphorylation results in the recruitment and activation of SYK, a protein tyrosine kinase (PTK) that initiates downstream events and amplifies the original BCR signal [13–16]. Although BCR signaling is generally thought to depend on ligand-induced aggregation, additional studies highlight the important role of "tonic" BCR maintenance or survival signals in the absence of receptor engagement [14, 17–19]. Lam et al. first demonstrated that the inducible loss of murine BCR resulted in the death of peripheral B cells, highlighting the requirement for continued BCR expression in viable B cells [18]. In follow-up studies, the selective excision of the Iga ITAM and ablation of Iga signaling led to the loss of mature B cells, further emphasizing the role of tonic BCR signaling in B-cell survival [17]. Consistent with its central role in the BCR signaling, SYK activity is tightly regulated by BCR-associated phosphorylation and Cbl-mediated proteasomal degradation. Additional studies highlight the likely role of PTPs in tonic BCR signaling, demonstrating that BCR-proximal PTKs can be activated by the phosphatase inhibitor pervanadate/H_2O_2 without BCR cross-linking [14, 15, 19, 20].

Several lines of evidence suggest that many B-cell lymphomas depend on B-cell receptor (BCR)–mediated survival signals as well. Most B-cell lymphomas retain BCR expression and limit immunoglobulin (Ig) loci translocations to nonproductively rearranged Ig alleles [21]. In addition, B-cell lymphomas with ongoing somatic hypermutation rarely exhibit loss of BCR expression [21]. Furthermore, treatment with anti-idiotypic antibodies uncommonly leads to the emergence of BCR-negative lymphoma variants [21]. Overexpression of multiple BCR signaling components including central regulator and amplifier of the cascade (SYK) in the "BCR"-type tumors, suggested that these tumors are more likely to be reliant on BCR pro-survival signaling.

BCL6 in DLBCL pathogenesis

BCL6 is a BTB/POZ domain transcription repressor that is the master regulator required for normal germinal center development and expressed by the majority of normal GC B cells and a subset of DLBCL [22, 23]. BCL6 favors the survival and proliferation of GC B cells, which undergo somatic hypermutation of Ig variable regions and Ig class switch recombination; down-regulation of BCL6 is necessary for post-GC B cell maturation [24–27]. Deregulation of BCL6, by chromosomal translocation or aberrant somatic hypermutation is the most common genetic abnormality in DLBCL [28]. Conclusive evidence for the oncogenic role of BCL6 comes from murine models in which constitutive BCL6 expression results in the development of a lymphoid malignancy resembling DLBCL [29, 30]. Although deregulated BCL6 clearly plays a pathogenetic role in a subset of human DLBCL, other DLBCL may simply express this transcriptional repressor because they are derived from normal BCL6+ GC B cells. Identification of BCL6-dependent tumors has important therapeutic implication because a recently described specific BCL6 peptide inhibitor (BPI) inhibits the growth of some but not all DLBCL [31, 32]. This inhibitor specifically inhibits recruitment of BCL6 corepressors such as BCoR, NCoR and SMRT, disrupts BCL6-mediated repression and establishment of silenced chromatin and reactivates natural BCL6 target genes. Intraperitoneal injection of BPI to mice prevent GC formation upon T-cell dependent antigen challenge, demonstrating that BPI abrogates BCL6 function *in vivo* and mimics BCL6 $^{-/-}$ phenotype [31].

Taken together, these observations suggested that the "BCR"-type comprehensive transcriptional signature is likely related to biological and functional foundations. It could be hypothesized therefore, that this specific molecular tumor category would be reliant on these pathways, and that

targeted inhibition of BCR signaling and/or BCL6 would be therapeutically beneficial. For these reasons, the studies were performed to investigate the specific aims as outlined below.

Aims of the study

1. To investigate the role of tonic pro survival SYK-dependent signaling in "BCR"-type DLBCL and biological consequences of its inhibition *in vitro*,
2. To investigate the mechanism controlling SYK activity,
3. To investigate the role of transcriptional program controlled by BCL6 and the biological consequences of its inhibition *in vitro*,
4. To explore the relationship between BCL6--mediated repression and SYK-dependent signaling in "BCR"-type DLBCL.

Material and Methods

Cell culture

The DLBCL cell lines DHL4, DHL6, DHL8, DHL10, Wsu-NHL, Karpas 422 (K422), OCI LY1, LY4, LY7, LY18, LY19, Pfeiffer, and Toledo were cultured in RPMI 1640 medium (Mediatech, Herndon, VA) supplemented with 10% fetal calf serum and 2 mM glutamine. DLBCL cell lines LY3 and LY10 were cultured in Iscove modified Dulbecco medium (IMDM) (Invitrogen, Grand Island, NY) supplemented with 20% human serum (Gemini Bio-Products,West Sacramento, CA) and 2 mM glutamine. All the cells were maintained at 37°C in 5%CO2. The cell lines, which were all mycoplasma-free, were obtained from the following sources: Pfeiffer and Toledo, American Tissue Culture Collection (ATCC, Manassas, VA); DHL4, DHL6, DHL8, DHL10, Wsu-NHL, Karpas422, Ly19, Deutsche Sammiung von Mikroorganismen und Zellkulturen GmbH (DSMZ, Braunschweig, Germany); and OCI Ly1, Ly3, Ly4, Ly7, Ly10, Ly18, Ontario Cancer Institute (University of Toronto, Toronto, ON).

Consensus cluster assignment to cell lines

The DLBCL cell lines were assigned to consensus clusters [9] using their transcriptional profiles and a recently described ensemble classifier which combines by majority voting the class assignments of 14 independent predictive algorithms [33, 34].

Treatment with R406

The small molecule SYK inhibitor, R406, [35] was a gift from Rigel (San Francisco, CA). R406 was dissolved in DMSO at a concentration of 10 mM and stored at -80°C. After thawing, the R406 stock solution was kept in a desiccator at room temperature for up to 1 week. DLBCL cell lines were treated with 1 or 4 μM R406 or vehicle alone for 72 hours.

Analysis of cellular proliferation and apoptosis

Cellular proliferation was determined by MTT assay (3-(4,5-dimethylthiazol-2-yl)-2,5-diphenyltetrazolium bromide) assay (Roche Diagnostics, Indianapolis, IN) using standard protocols. For each cell line, IC50 was calculated using GraphPad Prism 4 software (GraphPad Software, San Diego, CA). DLBCL cell line apoptosis was analyzed using annexin V-FITC/propidium iodide (PI) staining (Annexin V-FITC apoptosis detection KIT I; BD Biosciences, San Jose, CA). In these experiments, all cells were analyzed and the annexin V+, annexin V+/PI+ and PI+ cells were considered apoptotic.

Surface Ig cross-linking

Goat anti–human IgG was purchased from Jackson ImmunoResearch Laboratories (West Grove, PA). Cells (5×10^6) in 0.5 mL RPMI were stimulated with goat anti–human IgM and IgG for indicated periods of time.

Phospho-specific flow cytometry

Intracellular phospho-specific flow cytometry was performed as previously described [36] according to the manufacturer's instructions. In brief, 2×10^6 cells were resuspended in 1 mL cold PBS plus 1% FCS and left untreated or stimulated with goat anti–human IgG or IgM at 37°C as indicated. Thereafter, cells were fixed, permeabilized, and stained with the PE-conjugated a-pSYK (pY352 or pY348), PE-conjugated a-pBLNK (pY84) (BD Biosciences) or isotype control antibodies. Flow cytometric analysis was performed using a FACS Canto II flow cytometer (BD Biosciences).

DLBCL viable tumor cell suspensions

Using an institutional review board-approved protocol, freshly obtained nodal primary DLBCL specimens were minced over a wire mesh screen, washed, filtered and centrifuged over Ficoll Hypaque (Isolymph; Gallard-Schlesinger Industries, Garden City, NY) at 500 × g for 15 min. to isolate viable mononuclear tumor cells. Thereafter, the viable tumor cell suspensions were washed in RPMI, resuspended in DMSO and cryopreserved in liquid nitrogen. Prior to analysis, the tumor cell suspensions were thawed and viable cells were iso-

lated from a Ficoll Hypaque monolayer. The primary DLBCL tumor cell suspensions were analyzed by intracellular phosphospecific flow cytometry for pSYK (Y352) and pBLNK (pY84) at baseline, and following anti-IgG/IgM crosslinking in the presence or absence of R406, as described above.

Establishment of doxycycline-inducible PTPROt cell lines

The PTPROt-inducible lymphoma cell line was generated using a Tet-On Gene Expression System (BD Biosciences Clontech, Palo Alto, CA). In brief, the pTET-On regulatory plasmid was transfected into the lymphoma cell line, and several independent G418-resistant clones (0.75 mg/ml) were obtained. pTET-On–positive clones were screened for low background and high inducibility with pTRE2--Luc. Thereafter, selected clones were stably transfected with appropriate plasmids (pTRE2-PT--PROT-WT, pTRE2- PTPROT-C325S, or pTRE2--PTPROT-D291A) and selected with puromycin (at 1 μg/mL). The resulting transfectants were treated with doxycycline (1 μg/mL) for 12 hours at 37°C to induce PTPROt expression.

Immunoprecipitation and immunoblotting

Cells were lysed in NP40 lysis buffer (1% NP--40, 50mM Tris-HCl [pH7.4], 150mM NaCl, and 2mM Na_3VO_4) containing protease inhibitors. Following centrifugation, supernatants were recovered and used in immunoblotting or immunoprecipitations. For immunoprecipitations, lysates were incubated with 2 μg/mL a-SYK 4D10 or a-CD79a antibody (Santa Cruz Biotechnology) at 4°C for 1 h with rotation. Thereafter, 50 μL protein G–Sepharose beads (50% slurry in lysis buffer) was added, and samples were rotated for 1 additional hour. Immunocomplexes were then recovered by centrifugation, washed with cold lysis buffer, resuspended in sample buffer, boiled at 95°C for 10 minutes, size-fractionated by PAGE and transferred to PVDF membranes (Millipore Corp., Bedford, MA).

Blots were first incubated in blocking buffer (5% milk, 0.1% Tween in phosphate-buffered saline [PBS]) for 30 minutes and subsequently incubated 1 hr at room temperature or overnight at 4°C (phospho-specific or anti-pan-phospho-tyrosyl antibody). After sequential washes with 0.1% Tween/PBS, blots were incubated with horseradish peroxidase (HRP)–labeled secondary antibodies at room temperature for 1 hour, developed by enhanced chemiluminescence (Western Lighting Plus-ECL, PerkinElmer, Waltham, MA) and visualized with Kodak Biomax film (Carestream Health, Inc., Rochester, NY). To reprobe with another antibody, the blots were stripped (0.063 M Tris-HCl [pH 6.8], 2% SDS, 0.026 M DTT) at 50°C for 30 minutes, washed and analyzed with additional antibodies as indicated.

Antibodies used in immunoprecipitation and immunoblotting included mouse monoclonal antibody anti-SYK, and anti-BLNK, rabbit polyclonal antibody anti–extracellular signal–regulated kinase 1 (ERK1), (Santa Cruz Biotechnology, Santa Cruz, CA), anti–phospho-p44/42mitogen-activated protein kinase (MAPK) antibody (Cell Signaling Technology, Danvers, MA), SYK Y352 [BD Biosciences, San Jose, CA], Y525/526, Y323 [Cell Signaling, Danvers, MA], murine monoclonal anti–phospho-BLNK (pY84), mouse monoclonal antiphosphotyrosine antibody (4G10; Upstate, Lake Placid, NY), mouse monoclonal anti β-actin, and anti-FLAG antibody (Sigma, St Louis, MO).

Quantitative chromatin immunoprecipitation (QChIP)

Chromatin immunoprecipitations were performed as previously described using Ramos, DHL4 or DHL6 cells [31, 37–40]. Briefly, cells were fixed in 0.5% formaldehyde for 10 minutes at room temperature. Reactions were subsequently quenched in 0.2M glycine for 5 minutes. Cells were then washed with 1X PBS and lysed in RIPA lysis buffer (150 mM NaCl, 1% NP40, 0.5% sodium deoxycholate, 0.1% SDS, 50 mM Tris [pH 8.0], 2mM EDTA) containing protease inhibitors (Complete protease inhibitor cocktail; Roche Applied Science) and sonicated. Lysates were precleared and subsequently incubated with rabbit antisera directed against BCL6 (N3 antibody; Santa Cruz Biotechnology, Santa Cruz, CA) or with normal rabbit IgG antibody (Santa Cruz Biotechnology). Immunocomplexes were captured with protein A/G Plus agarose pre-blocked with salmon sperm DNA (Abcam, Cambridge, MA) and washed 3 times with RIPA buffer and once with final ChiP wash buffer (1% NP40, 0.1% SDS, 500 mM NaCl , 2mM EDTA, pH 8.0, 20mM Tris--HCl, pH 8.0, with protease inhibitors). Thereafter, immune complexes were eluted with 1% SDS in 100 mM $NaHCO_3$ and crosslinks were reversed by incubating samples for 4h at 65°C. Samples were then digested with Proteinase K for 1h at 45°C. DNA fragments enriched by ChIP were recovered by standard phenol-chloroform extraction followed by ethanol precipitation and quantified by real-time PCR and PowerSYBR green kit (Applied Biosystems, Foster City, CA). Relative enrichment in BCL6 binding sites and control regions in BCL6--over control IgG-immunoprecipitated samples was

calculated by using the $2^{-(\Delta CT\ BCL6\ -\ \Delta CT\ IgG)}$ method. Standard deviations were calculated from triplicate ΔΔCT values. The known BCL6 binding sites in the *CCL3 and FCER2* genes [41, 42] were used as positive controls for BCL6 target gene enrichment while the CD20 gene, which is not a BCL6 target, was used as a negative control. Primers used in these experiments are available upon request.

ChIP on chip and data processing

After validation of enrichment by QPCR, BCL6 or actin ChIP products and their respective input genomic fragments were amplified by ligation-mediated PCR (LMPCR) [43]. QChIP was repeated after amplification to verify that the enrichment ratios were retained. The genomic products of three biological ChIP replicates were labeled with Cy5 (for ChIP products) and Cy3 (for input) and co-hybridized on a NimbleGen human promoter array representing 1.5 KB of promoter sequence from 24.275 genes (human genome v. 35, May 2004) according to manufacturer's protocol (NimbleGen Systems, Madison, WI). The enrichment for each promoter was calculated by computing the log-ratio between the probe intensities of the ChIP product and input chromatin, which are co-hybridized on the same array. Thereafter, for each of the 24,175 promoter regions, the maximum average log-ratio of three neighboring probes in a sliding window was calculated and compared with random permutation of the log-ratios of all probes across the entire array. The positive threshold was defined using the *CCL3* signal that corresponds to the 95th percentile in random permutation of the log-ratios. The putative BCL6 binding regions were calculated from triplicate experiments, represented as enrichment peaks of BCL6 over control antibody signal and aligned with chromosome positions (NCBI human genome assembly v.35, May 2004). Thereafter, using NimbleGen 24K promoter array annotation file, the peak signals of BCL6 binding were assigned to the respective regulatory regions of candidate BCL6 target genes. In addition, all peaks were inspected using BLAT (The BLAST-like Alignment Tool, http://genome.ucsc.edu) to identify genes on opposite strand that could be regulated from the same bidirectional promoter. Two genes were considered to be bidirectional partners when they were located on the opposite strands in a "head-to-head" orientation and their transcription start sites were separated by less than 1kb [44]. In previous studies, 90% of promoters meeting these criteria were bidirectionally active in functional assays [44, 45].

Gene Ontology Term Enrichment Analysis

Gene Ontology (GO) term enrichment analysis was performed with the online version of GeneMerge program (http://www.oeb.harvard.edu/hartl/lab/publications/GeneMerge GeneMerge.html [46]). Enrichment was assessed by comparing frequency of GO Biological Process categories (http://www. geneontology.org/GO.doc.shtml) represented in the non-redundant list of SwissProt/TrEMBL accession numbers of BCL6 target genes (n = 418) *versus* the global frequency of GO categories in the population gene file containing 19,168 non-redundant SwissProt/TrEMBL accession numbers which corresponded to known genes in NCBI human genome assembly v.36 (March 2006). SwissProt/TrEMBL IDs of remaining BCL6 target loci were not available. All SwissProt/TrEMBL IDs were obtained from the Affymetrix genome annotation file supporting U133 Plus 2 GeneChip (ver. July 2006). Obtained p-values were corrected for multiple hypothesis testing by FDR (False Discovery Rate) [47, 48].

Gene Set Enrichment Analysis

Gene Set Enrichment Analysis (GSEA) was performed using the GSEA v1.0 program (available from http://www.broad.mit.edu/gsea) [49], the BCL6 target gene set and 2 independent series of primary DLBCL with gene expression profiles and consensus cluster and COO designations [9, 10]. Since the signature of the "HR" tumors is largely defined by normal tumor-infiltrating host inflammatory and immune cells, the analysis was focused on "BCR" and "OxP" DLBCL. GSEA was performed as previously described, with minor modifications. The top 15,000 genes selected with a MAD-based variation-filter were first ranked with respect to the phenotype, "BCR" *vs.* "non-BCR", using an absolute value (rather than positive or negative) signal-to-noise ratio (SNR). With this approach, the final position in the ranked gene list was only dependent on the strength of the gene in discriminating between phenotypes rather than specific up- or down-regulation in a given phenotype. Represented members of the BCL6 target gene set were then located within the ranked gene list and the proximity of the BCL6 target gene set to the most differentially expressed "BCR" *vs.* "non-BCR" genes (*i.e.*, those with the highest absolute SNR value) was measured with a weighted Kolmogorov-Smirnov statistic (ES, enrichment score [49]), with a higher score corresponding to a higher proximity. The observed ES score was then compared to the distribution of 1000 permuted ES scores (gene

tag permutations) to assess statistical significance. Similar results were observed with the permutation of the class template (data not shown). The query gene set included the 309 (out of total 485) BCL6 target genes present in the 15,000 ranked genes; these 309 BCL6 targets were represented by 477 Affymetrix probe sets. BCL6 target gene enrichment was also assessed in the gene list ranked for the positively defined COO phenotypes "GC" *vs.* "ABC" [9, 11] sorted by absolute SNRs.

GSEA was also performed in an independent dataset of 218 primary DLBCL patients with available COO designations http://llmpp.nih.gov/DLBCL/DLBCL_patient_data_NEW.txt [10] and consensus cluster assignments [9]. Affymetrix IDs of BCL6 target genes were translated to Lymphochip IDs using current and archival UniGene cluster IDs and used as the query gene set. Enrichment was assessed as described above by ranking the genes with respect to the absolute SNR values for the comprehensive cluster phenotypes "BCR" *vs.* "non-BCR" or COO phenotypes "GC" *vs.* "ABC".

The top-scoring BCL6 target genes, described as the "leading edge" genes, appear in the ranked list at or before the point where the ES running sum reaches its maximum deviation from zero [49]. The leading-edge genes can be interpreted as the core of a gene set that accounts for the enrichment signal [49]. These top-scoring BCL6 target genes were clustered with respect to the "BCR" *vs.* "non-BCR" tumor phenotypes and represented on heat maps using the dChip 2006 program. For comparison, the heat maps also included normal $CD19^+$ $sIgD^-$ $CD38^+$ GC B cells that were isolated as previously described [50] and transcriptionally profiled at the same time as the primary DLBCL [9].

GSEA in cell lines

Total RNA was extracted from a panel of DLBCL cell lines, processed, hybridized to U133A and B Affymetrix oligonucleotide microarrays, scanned and analyzed as previously described [9]. Cell lines were then assigned to consensus clusters using an ensemble classifier incorporating multiple independent predictors as described above. Cell lines that were assigned to "BCR" or "non-BCR" categories with the highest probability were selected for GSEA and additional functional analyses. GSEA was performed as described above, using the top 12,666 genes that met threshold and variation index criteria [45]; genes were ranked according to the absolute SNR values for the phenotype "BCR" *vs.* "non-BCR". The proximity of the BCL6 target gene set to the top of the ranked list was measured with an ES and the significance of the ES was determined using 1000 gene tag permutations, as described above.

Treatment with BCL6 inhibitory peptide

Peptides, including BCL6 inhibitory peptide (BPI) and control were obtained from Bio-Synthesis Inc. (Lewisville, TX) and stored at –20°C until reconstituted with sterile pure water immediately before use [32]. BPI purity was determined by HPLC-MS to be 98% or higher. 25×10^4 DLBCL cells were exposed to BPI or control peptide (0, 1, 2.5, 5, 10, 20, 40 and 80 μM) every 24 hrs. for 48 hrs. Cellular proliferation was assessed by MTT assay as described above using 8 replicates per treatment condition. The proliferation of BPI-treated cells (T) was normalized to their respective controls (C) as follows: $(T/C)_{corr}\,(\%) = (T/C)\,/\,UT \times 100$. The growth inhibition (IC50) values were estimated by a linear least-squares regression of the $(T/C)_{corr}$ values versus the concentration of BPI (or control) peptide; T/C_{corr} values of 50% were extrapolated. The difference in BPI IC50s of "BCR" and "non-BCR" cell lines was assessed with a two-sided Student *t*-test.

BCL6 target gene expression

After treatment with 20 mM of BPI or control peptide for 8 hours, RNA was extracted from 10^4 DLBCL cells, using the RNeasy kit (Qiagen, Valencia, CA). cDNA was synthesized using Superscript III First Strand cDNA Synthesis kit (Invitrogen, Carlsbad, CA). The mRNA levels of SUB1, CBX3, CR1, ZNF433, CCN1, MBD1, CD74, FCER2 and HPRT (housekeeping control) were detected using the SYBRgreen kit (Applied Biosystems) and an Opticon Engine 2 thermal cycler (MJ Research). Primer sequences for QPCR are available upon request. The C_T values of the genes of interest were normalized to HPRT (ΔC_T). ΔC_T values of the BPI-treated cells were expressed relative to control peptide-treated cells using the $\Delta\Delta C_T$ method. The fold change in expression of each gene in BPI-treated vs. control peptide-treated cells was determined by the expression: $2^{-\Delta\Delta CT}$ with $\Delta\Delta C_T$ +s and $\Delta\Delta C_T$ –s where s is the standard deviation of the $\Delta\Delta C_T$ value for triplicates. Results were represented as fold expression with standard deviation.

Microarray analysis of BCL6 and PTPRO in normal B cells and in tumor samples

Two previously described datasets of transcriptionally profiled newly diagnosed DLBCL [9, 10] and an additional series of profiled normal B-cell sub-

sets (naïve, centroblasts, centrocytes, and memory cells) [51] were used to assess BCL6 and PTPROt transcript abundance. An additional series of highly purified normal B-cell subsets (naïve, centroblasts, centrocytes, and memory cells) was isolated from normal human tonsils by magnetic cell separation (MidiMACS system, Miltenyi Biotec, Auburn, CA) and profiled using the Affymetrix U133Plus platform as previously described [52]. Affymetrix probes 208121_s_at (PTPRO), 203140_at, 215990_s_at (BCL6) and dChip 2007 program were used to assess PTPROt and BCL6 transcript abundance in the Monti et al. [9] dataset; for lymphochip [10] dataset, the following probes were used: 17772 (PTPRO), 26535, 24429, 19268 (BCL6).

Computational analysis of PTPROt promoter, generation of PTPROt promoter constructs and luciferase assays

Computational analysis of *PTPROt* promoter was performed with the publicly available MatInspector module of Genomatix suite (http://www.genomatix.de). The ~1.6 kb sequence spanning –1.1 kb upstream to +0.5 kb downstream from previously identified *PTPROt* transcription start site (TSS) [50] was interrogated and three putative BCL6 binding sites were identified. To generate a PTPROt promoter reporter construct, a fragment spanning nucleotides –1108 to +381 was PCR-amplified and cloned into the promoterless pGL3 luciferase vector (Promega, Madison, WI). Deletions in BCL6 binding sites were generated using the GeneTailor Site-Directed Mutagenesis System (Invitrogen, Carlsbad, CA) as recommended by the manufacturer. BCL6 constructs encoding either the wild type protein (pMT2T-HA-BCL6) or mutant protein, lacking N-terminal POZ domain or C-terminal zinc fingers, (pMT2T-HA-BCL6-ZF and pMT2T-HA-BCL6-ΔZF, respectively) were utilized [37].

For luciferase assays, HEK293T cells were maintained in Dulbecco-modified Eagle's medium (Cellgro Mediatech, Herndon, VA) supplemented with 10% fetal calf serum (Cellgro Mediatech), 10 mM HEPES buffer, 4 mM L-glutamine, 50 U/mL penicillin and 50 U/mL streptomycin. HEK293T cells were seeded on 6 well-plates, grown to 60–80% confluency and cotransfected with 350 ng/well of the appropriate promoter pGL3 construct (wild-type or mutant *PTPROt* promoter construct), 150 ng/well of the control reporter plasmid, pRL-TK (Promega) and 5–100 ng of wild-type or mutant BCL6 construct using FuGENE 6 transfection reagent (Roche Applied Science, Indianapolis, IN) according to manufacturer's protocol. After 24 h of incubation, cells were lysed and luciferase activities were determined by chemoluminescence assay using the Dual Luciferase Assay kit (Promega) and Luminoskan Ascent luminometer (Thermo Lab Systems, Franklin, MA). Luciferase activities are presented as means from 3 experiments ± SD.

Analysis of BCL6-mediated PTPROt repression in normal tonsillar naïve B-cells and centroblasts

Normal naïve B-cells and centroblasts were obtained from human tonsils by magnetic cell separation with the MidiMACS system (Miltenyi Biotec) as previously described [52]. Expression of the BCL6 construct in naive B cells was achieved by infection of the cells with a FUGW lentivirus vector (Addgene, Cambridge, MA) expressing BCL6 or an EGFP-only control as previously described [52]. For BCL6 knockdown in centroblasts, BCL6-specific or a negative control "scrambled" shRNA cloned into the pFIV-H1-copGFP vector were used [50].Following 48h, total RNA was prepared with TRIzol (Invitrogen) and reverse-transcribed to cDNA with the Superscript III first-strand cDNA synthesis kit (Invitrogen). PTPROt transcript abundance was evaluated by quantitative 5'-nuclease assay PCR with the following primers and 5'-FAM labeled MGB probe: Forward: ACTTTGTCTTTGCTCAGAACCAG; Reverse: AGAAACAGCAACTGGTTCCTGAAG; probe: CACTCTTCGCAGTGAAC. PCR was performed using an ABI 7700 thermal cycler (Applied Biosystems) and threshold cycle (C_T) values were generated using the Sequence Detection Software, version 1.2 (Applied Biosystems). PTPROt transcript abundance was calculated relative to the housekeeping control cyclophilin A (Applied Biosystems, cat. no 4326316E) using the $2^{-(\Delta CT\ PTPROt\ -\ \Delta CT\ PPIA1)}$ method. Standard deviations were calculated from triplicate $\Delta\Delta CT$ values. For absolute mRNA copy number quantification, PCR was performed with a serial dilutions of plasmid DNA containing the PCR target sequence. CT values from the serial dilutions were plotted against log (# plasmid copies) to generate standard curves as described previously [45]. Expression of the control BCL6 target gene, FCER2, was assessed relative to GAPDH by using RT-PCR, PowerSYBR Green kit and the following primers: FCER2, F: ATGAATCCTCCAAGCAGGAG, FCER2, R: GACTTGAAGCTGCTCAGACTGCT; GAPDH, F: GATTCCACCCATGGCAAATTC; GAPDH, R: TGATTTTGGAGGGATCTCGCTC.

RNA-interference mediated BCL6 knock-down

BCL6-specific onTARGET plus siRNA and negative control scrambled oligo (CCUCCAUAUCUCGCGCGUCUU) were obtained form Thermo Scientific (Thermo Scientific, Waltham, MA). Oligos were resuspended in RNAse-free water at 50 mM and stored at –70°C. For siRNA nucleofections, 4 x 10^6 of DHL4 cells were resuspended in 100 mL of AMAXA nucleofector solution V containing 75 pmoles of BCL6 or SCR oligo and treated with O–017 program in Nucleofector II device (AMAXA, Koeln, Germany). Transduction efficiency was confirmed to be above 90% by nucleofection of Cy3-labeled GAPDH oligo (Applied Biosystems/Ambion, Austin, TX) and subsequent flow cytometry analysis. After nucleofections, DHL4 cells were incubated for 72h and used for phospho-specific flow cytometry, or to prepare whole-cell extracts (WCE) for immunobloting or for immunoprecipitations.

Immunoblot analysis of SYK and BLNK phosphorylations following BCL6 knockdown

Whole–cell extracts from BCL6 siRNA-transduced cells were obtained by directly lysing cells in the RIPA lysis buffer. For immunoprecipitations, cells were first resuspended in 150 mL of PBS containing 1% FCS and left untreated or stimulated with goat anti–human IgG at 37°C for 1 minute as described above. Cell suspensions were immediately lysed in 150mL of 2x NP40 lysis buffer (2% NP-40, 100 mM Tris-HCl [pH7.4], 300 mM NaCl, 4 mM Na_3VO_4 with protease inhibitors) and immunoprecipitations with a-SYK were performed as described above. Lysates or immunoprecipitates were size-fractionated on NuPAGE Novex 4–12% Bis-Tris Gels (Invitrogen), and transferred to PVDF membranes (Millipore). Blots were incubated with primary antibodies, washed, incubated with appropriate HRP–labeled secondary antibodies, developed and visualized as described above.

Results

1. Constitutive SYK-dependent tonic B-cell receptor signaling is a survival pathway in the "BCR" molecular type of diffuse large B-cell lymphomas

1.1. An ATP-competitive, specific inhibitor of SYK (R406) inhibits proliferation and induces apoptosis of "BCR"-type DLBCL cell lines

To investigate the postulated pro-survival role of tonic BCR signaling in DLBCL, the effect of the SYK inhibitor (R406) on the cellular proliferation of a large panel of DLBCL cell lines was assessed. These DLBCL were treated with serial dilutions of R406 or vehicle alone and proliferation was evaluated thereafter by MTT assay. In the majority of the DLBCL cell lines, R406 inhibited cellular proliferation at IC50s ranging from 0.8 μM to 8.1 μM (data not shown and [33]). R406 cytotoxicity to DLBCL was next evaluated using 2 doses of the SYK inhibitor, 1 μM and 4 μM, derived from the IC50 analysis. The DLBCL were cultured with R406 or vehicle alone and assessed for apoptosis by annexin V–FITC/propidium iodide (PI) staining. Ten of the DLBCL cell lines exhibited high levels of apoptosis following R406 treatment (Figure 1, left panel), whereas 5 lines did not undergo R406-associated apoptosis (Figure 1, right panel). Of interest, all of the R406-sensitive cell lines were previously designated "BCR-type" DLBCL using the cell line transcriptional profiles and a recently described ensemble classifier [33, 34] (Figure 1, left panel). In contrast, none of the R406-insensitive cell lines were identified as "BCR-type" tumors (Figure 1, right panel). Taken together, these data suggest that transcriptional profile-defined "BCR-type" DLBCL may be uniquely reliant on BCR-mediated survival signals.

1.2. "BCR" type cell lines exhibit tonic BCR activity that can be specifically inhibited with R406

SYK activation requires LYN-mediated phosphorylation of SYK Y352 and Y348 in the linker region followed by autophosphorylation of SYK Y525/526 in the catalytic domain (Figure 2A). Subsequent phosphorylation of SYK Y323 leads to Cbl-mediated ubiquitylation and degradation of SYK. Given the critical role of SYK in low-level tonic BCR signaling, a highly sensitive, recently described method of single-cell phospho-flow cytometry was used to assess SYK phosphorylation and signaling in the DLBCL cell lines in the absence of BCR crosslinking [36, 53]. With this approach, it is possible to precisely quantitate SYK activation by measuring phospho-SYK348, -SYK352, and -BLNK expression in DLBCL before and after BCR engagement (Figure 2). Of interest, all of the "BCR-type" DLBCL cell lines exhibited immunodetectable tonic phosphorylation of SYK348 and SYK352 and the majority of these lines also had lower but detectable baseline phospho-BLNK (Figure 2B). As expected, SYK348, SYK352, and BLNK phosphorylation markedly increased following BCR crosslinking in these DLBCL (Figure 2B). Only 2 of 5 "non-BCR"

DLBCL cell lines exhibited tonic phosphorylation of SYK348 and SYK352 and none of these lines had evidence of tonic phospho-BLNK (Figure 2C). After documenting SYK and BLNK phosphorylation in R406-sensitive DLBCL in the absence of Ig crosslinking, the effects of R406 on tonic BCR signaling was assessed. Since R406 specifically inhibits its SYK525/526 autophosphorylation and downstream signaling events including the phosphorylation of BLNK [33], R406-sensitive DLBCL cell lines were treated with R406 or vehicle alone, and tonic pBLNK levels were evaluated in the absence of Ig crosslinking (Figure 3). As indicated, R406 treatment markedly reduced tonic BLNK phosphorylation (Figure 3).

1.3. R406 inhibits BCR signaling in a subset of primary DLBCL

After demonstrating that R406 sensitivity was dependent on intact BCR signaling in DLBCL cell lines, the same parameters were evaluated in viable tumor cell suspensions from 10 primary DLBCL. Prior to these experiments, surface Ig isotype was determined by flow cytometry (data not shown and [33]) and subsequently, pSYK352 and pBLNK expression at baseline and following BCR crosslinking were compared in the presence or absence of R406. Five representative primary DLBCL are shown in Figure 4. In the majority of examined primary DLBCL, the tumor cells expressed clearly detectable pSYK352 at baseline (Figure 4A, top panel). In each of these viable tumor cell samples, BCR crosslinking markedly increased SYK352 and BLNK tyrosyl phosphorylation (Figure 4A, top panel). Furthermore, R406 inhibited the SYK-dependent phosphorylation of BLNK following BCR engagement (Figure 4A, bottom panel). In marked contrast, other primary DLBCL had no or low levels of detectable pSYK352 at baseline (Figure 4B, top panel). In these primary DLBCL, there was no change in pSYK352 and pBLNK levels following BCR crosslinking (Figure 4B, top panel) and R406 had no observed effect (Figure 4B, bottom panel). These analyses of primary DLBCL which are in agreement with those of DLBCL cell lines (Figures 2–3), indicate that primary DLBCL also differ in their tonic and induced BCR signaling and sensitivity to R406.

2. Identification of the phosphatase — dependent mechanism controlling SYK activity

Consistent with the central role of SYK in regulating tonic and ligand-dependent BCR signaling, SYK activity is tightly regulated by BCR-associated phosphorylation, Cbl-mediated proteasomal degradation and PTP activity. Pilot studies suggested that SYK activity could be controlled by a tissue-specific and developmentally regulated PTP, PTPROt (Protein Tyrosine Phosphatase Receptor Type O, truncated) [54]. PTPROt coimmunoprecipitaded with SYK, indicating that these proteins form a complex. In addition, the substrate-trapping mutants of PTPROt that lack catalytic activity, but retain the ability to bind substrates, bound significantly more tyrosyl-phosphorylated and total SYK than wild-type PTPROt (PTPROt-WT), suggesting that SYK could be a PTPROt substrate *in vivo*.

2.1. Characterization of PTPROt role in dephosphorylating SYK Y352 *in vivo*

To furher characterize PTPROt substrates *in vivo*, tet-inducible B-cell lines that expressed either WT or CS mutant FLAG-tagged PTPROt were used. If SYK is a PTPROt substrate, overexpression of WT PTPROt would inhibit BCR-triggered SYK tyrosyl phosphorylation. SYK activation requires LYN-mediated phosphorylation of SYK Y352 and Y348 in the linker region followed by autophosphorylation of SYK Y525/526 in the catalytic domain (Figure 2A). Subsequent phosphorylation of SYK Y323 leads to Cbl-mediated ubiquitylation and degradation of SYK. To confirm that SYK is a PTPROt substrate and identify specific PTPROt SYK tyrosine substrate, Flag-tagged WT or CS mutant PTPROt were overexpressed in DLBCL cells, BCR was crosslinked for 5 min and BCR-induced phosphorylation at SYK Y352, Y525/526 and Y323 were compared (Figure 5A). At this early timepoint, SYK Y352 phosphorylation was specifically inhibited by overexpression of WT-PTPROt, but not by the inactive CS-PTPROt mutant (Figure 5A). In the same experiments, WT-PTPROt overexpression did not alter the phosphorylation of upstream BCR pathway components such as CD79a (Iga) (Figure 5A, bottom panel). To assess the effects of PTPROt on the subsequent phosphorylation of SYK Y525/526 and Y323, the same experiments following 15 minutes of BCR crosslinking were performed (Figure 5B). At this later timepoint, when phosphorylation of all three SYK tyrosine residues is detectable, overexpression of WT-PTPROt, but not CS-PTPROt, inhibited phosphorylation of SYK Y352, Y525/526 and Y323 (Figure 5B). Taken together, these results indicate that PTPROt dephosphorylates SYK Y352, limiting subsequent SYK Y525/526 autophosphorylation and activation of the BCR pathway.

2.2. PTPROt overexpression inhibits SYK--dependent MAPK/ERK signaling, cellular proliferation and induces apoptosis

Given the central role of SYK in transducing, amplifying and propagating the original signal to the downstream components of the BCR signaling pathway, it was likely that PTPROt overexpression would alter the phosphorylation of downstream SYK targets and associated cellular proliferation. Since the MAPK/ERK signaling pathway is one of the most important downstream signaling pathways regulated by SYK [55, 56], the phosphorylation of ERK1/2 in Dox-induced PTPROt-WT and mutant transfectants was investigated. ERK1/2 was strongly phosphorylated after BCR cross-linking (Figure 6, lane 2), and ERK1/2 phosphorylation was significantly inhibited by PTPROt-WT overexpression (Figure 6; compare lanes 2 and 4). In contrast, overexpression of PTPROt-CS or -DA mutants had little effect on ERK1/2 phosphorylation (Figure 6, lanes 8 and 12). Given the role of the MAPK/ERK signaling pathway in regulating cellular proliferation [57], the effect of PTPROt overexpression on cell growth using an MTT assay was next examined. Cellular proliferation was completely inhibited when PTPROt-WT transfectants were induced with Dox, although these cells grew normally in the absence of Dox (and PTPROt-WT expression) (Figure 7A, left panel). In marked contrast, cellular proliferation was not significantly altered by the induction of either PTPROt mutant (DA, CS) (Figure 7A, middle and right panels). In companion experiments, the effect of PTPROt overexpression on cellular apoptosis was assessed with annexin V–FITC/PI staining. Dox-induced PTPROt-WT dramatically increased the apoptotic cell fraction, whereas neither PTPROt mutant (DA or CS) had this effect (Figure 7B; compare left *vs.* middle/right panels).

3. Identification of BCL6-dependent, functional signature of "BCR" type DLBCL

The first part of studies demonstrated that that the molecular signature of "BCR"-type DLBCL has strong biological foundations in constitutive tonic BCR activity that is controlled by the PTPROt activity and therapeutically targetable. As the "BCR" molecular signature includes increased expression of BCL6, it was likely that deregulated expression of this proto-oncogene would have similar biological imprint. Specifically, these characteristics prompted speculations that "BCR" tumors would have a transcriptional signature that was defined, at least in part, by the differential expression of BCL6 target genes, and be more likely to rely upon deregulated BCL6 expression and be uniquely sensitive to BCL6 inhibition.

3.1. Identification and functional characterization of BCL6 target genes

To investigate these hypotheses, a comprehensive, BCL6-driven genetic signature was required. To identify BCL6 target genes, high throughput chromatin immunoprecipitation (ChIP on chip) was performed. Ramos B-cell lymphoma cell line which is frequently used to evaluate BCL6 function was utilized for these experiments [37–39]. Chromatin fragments were immunoprecipitated with an antibody directed against BCL6 or an irrelevant control. Thereafter, the resulting amplicons were labeled and co-hybridized with input chromatin to high-density oligonucleotide arrays containing 1.5 KB sequence of 24,275 gene promoters. "Hits" were captured through a highly stringent approach employing random permutation analysis on a sliding window of oligonucleotide probes (*i.e.* on groups of three consecutive probes). The threshold of positivity was set at the enrichment level of the known BCL6 binding site in the *CCL3* promoter [41], which corresponded to the 95th percentile confidence interval for this method. Only genes that were captured by all three replicates and that displayed overlapping peak enrichment were considered positive.

BCL6 was recruited to 436 promoters, potentially regulating 485 target genes, including known target genes such as *FCER2* and *CCL3* [41, 42] (The complete list of genes is available at the following URL: http://www.pnas.org/content/suppl/ /2007/02/13/ 0611399104.DC1/11399Table_2.pdf) To determine the accuracy of BCL6 target gene discovery, single locus quantitative ChIP was performed on 54 of the candidate BCL6 target genes using the known targets *CCL3* and *FCER2* as positive controls. Eighty-one percent of the examined candidate BCL6 target genes were confirmed with this stringent approach (Figure 8).

To gain insights into the functions of identified BCL6 target genes, their associated GO Biological Process terms were evaluated. GO terms annotate genes and their products based on described biological functions. Specifically, the representation of GO terms in the BCL6 target gene set with that in the total analyzed gene pool (*i.e.* all the genes in the GO database) was compared [46]. The BCL6 target gene list was enriched in genes regulating transcrip-

Table 1. Gene Ontology (GO) term analysis of BCL6 target genes

GO Term	GO term frequency in BCL6 target gene set	Global GO term frequency	P value	FDR
Transcription	37/418 (0.0885)	0.0386	0.0000	0.0003
Protein ubiquitination	15/418 (0.0359)	0.0096	0.0000	0.0006
Cell cycle	14/418 (0.0335)	0.0103	0.0001	0.0035
Ubiquitin cycle	12/418 (0.0287)	0.0083	0.0002	0.0043
Chromatin modification	6/418 (0.0144)	0.0023	0.0003	0.0053
Response to DNA damage stimulus	3/418 (0.0072)	0.0004	0.0004	0.0053
Regulation of transcription, DNA-dependent	41/418 (0.0981)	0.0567	0.0005	0.006
Ubiquitin-dependent protein catabolism	7/418 (0.0167)	0.0039	0.0011	0.013

tion, DNA damage responses, chromatin modification, cell cycle and protein ubiquitylation (Table 1).

3.2. Differential BCL6 target gene expression in DLBCL subtypes

It could be predicted that differential expression of BCL6 target genes would identify DLBCL in which BCL6 plays a dominant oncogenic role and assessed the relative abundance of BCL6 targets in the respective DLBCL consensus clusters [9]. In this analysis, gene set enrichment analysis (GSEA) was used to determine whether the set of BCL6 target genes was differentially expressed in a specific DLBCL subtype [49]. Although BCL6 likely functions as a direct transcriptional repressor, the absolute levels of specific target genes may depend upon BCL6 cooperation with other transcription factors, binding to different co-repressors, or additional epigenetic modifications of chromatin. For these reasons, phenotype ranking was performed according to absolute (rather than positive or negative) signal to noise ratios (SNR) and the enrichment of BCL6 target genes in the ranked dataset was assessed. In the series of 176 primary DLBCL, the "BCR" *vs.* "non-BCR" ranked gene list was significantly enriched for BCL6 target genes ($p < .0001$), indicating that the BCL6 signature contributes to the difference between "BCR" and "non-BCR" tumors.

To validate these observations in an independent dataset, GSEA was performed in an additional large series of transcriptionally profiled primary DLBCL with available COO and consensus cluster designations [9, 10]. In this independent series, BCL6 targets were similarly enriched in ranked genes discriminating between "BCR" and "non-BCR" signatures ($p = 0.017$). In contrast, BCL6 target genes were not significantly enriched in either dataset when the DLBCL were sorted with respect to the "GCB" *vs.* "ABC" classification.

To determine which BCL6 targets were more (or less) abundant in "BCR" *vs.* "non-BCR" DLBCL, the BCL6 target genes were clustered with respect to these tumor types. The top-scoring BCL6 target genes ("the leading edge" [see Methods] [49]) were represented on a heat map that included normal tonsillar GC B cells for comparison (Figure 9A). Consistent with the known role of BCL6 as a transcriptional repressor, a number of BCL6 target transcripts were less abundant in "BCR" DLBCL than in "non-BCR" tumors (Figure 9A); the majority of these BCL6 targets were also less abundant in normal GC B cells (Figure 9A). However, additional *bona fide* BCL6 targets were more abundant in "BCR" tumors and normal GC B cells than "non-BCR" DLBCL (Figure 9A). To explain this unexpected observation, the BCL6 dependence of candidate target genes in a panel of informative DLBCL cell lines was analyzed.

3.3. BCL6 actively represses its target genes in "BCR" but not in "non-BCR" tumors

For these analyses, representative "BCR" or "non-BCR" DLBCL cell lines ("BCR" — Ly1, Ly7, SU-DHL4, SU-DHL6 and Farage; and "non-BCR" — Ly4, Toledo, Karpas 422 and Pfeiffer) were used. The above phenotype assignment was based on the cell transcriptional profiles and an "ensemble classifier" (see Materials and Methods). Thereafter, GSEA was performed for BCL6 targets using the cell line gene list, ranked according to absolute SNR values for the "BCR" *vs.* "non-BCR" distinction. As was the case in primary DLBCL, BCL6 target genes were highly enriched in the ranked cell line gene

list ($p < .001$). In addition, certain BCL6 target transcripts were less abundant in "BCR" than in "non-BCR" cell lines whereas other BCL6 targets were more abundant in "BCR" DLBCL (Figure 9B).

Then, the panel of four "BCR" and "non-BCR" cell lines was treated with BPI and the transcript abundance of representative BCL6 targets was valuated (Figure 9C). The BCL6 targets chosen for this analysis were: (1) validated by Q-ChIP; (2) included in a significantly enriched GO category; and (3) most differentially expressed in "BCR" and "non-BCR" tumors (*i.e.* included in the leading edge gene set). Specifically, selected genes included certain candidate BCL6 targets that were less abundant in "BCR" than in "non-BCR" cells (SUB1, ZNF443, CR1, CBX3) at baseline (shaded in blue in Figure 9C), and others that were more abundant in "BCR" tumors (CD74, CCN1, MBD1, FCER2) (shaded in red in Figure 9C). BPI treatment increased the expression of each of these BCL6 targets in the "BCR" DLBCL cell lines but did not alter the expression of these genes in "non-BCR" tumors (Figure 9C). These data suggest that BCL6 is biologically active in "BCR", but not in "non-BCR", tumors and show that BCL6 represses its target genes in "BCR" DLBCL regardless of their baseline levels.

3.4. Disruption of the BCL6 transcriptional program selectively inhibits proliferation of "BCR"-type DLBCL cell lines

Since BPI selectively increased BCL6 target expression in "BCR" DLBCL, it could be predicted that these tumors would be more dependent on BCL6-regulated gene pathways than "non-BCR" DLBCL. It had been previously shown that BPI specifically blocked BCL6 activities *in vitro* and *in vivo* and inhibited the growth of certain BCL6-positive lymphomas [31]. For this reason, the 5 "BCR" and 4 "non-BCR" DLBCL cell lines were treated with BPI and tumor cell proliferation was subsequently evaluated. In these experiments, cell line identity was blinded until after the functional data were independently analyzed.

"BCR" cell lines had significantly lower BPI IC50s than "non-BCR" lines, which were uniformly resistant to the peptide inhibitor ("BCR" *vs.* "non-BCR" DLBCL IC50, 12.7 ± 3.49 mM *vs.* 50.15 ± 4.43 mM, $p < .0001$, Figure 10 A & B). To further characterize the differential sensitivity of "BCR" *vs.* "non-BCR" cell lines, the panel was exposed to 20 mM BPI for 48 hrs. BPI inhibited cellular proliferation of "BCR" DLBCL cell lines by 65–90% but had little effect on "non-BCR" tumors (Figure 10C).

4. Characterization of BCL6 role in tonic BCR signaling in DLBCL

Since the same transcriptionally defined subset of DLBCL relies upon SYK-dependent BCR signaling and exhibits coordinate BCL6-mediated transcriptional repression, the relationship between these two processes was explored.

4.1. Reciprocal patterns of PTPROt and BCL6 expression in normal B cells and primary DLBCL

To identify putative BCL6 target genes involved in BCR signaling, the relative expression of multiple proximal components of BCR signaling cascade and BCL6 was first compared. PTPROt and BCL6 exhibited reciprocal expression pattern in 2 independent series of highly purified naïve, GC and memory B cells analyzed by transcriptional profiling (Figure 11A). Consistent with BCL6 transcriptional repressor function, PTPROt transcripts were significantly more abundant in normal naïve and memory B cells than in GC B cells whereas BCL6 expression was highest in normal GC B cells (Figure 11A). In addition, there were reciprocal patterns of BCL6 and PTPROt expression in 2 large independent series of primary DLBCL (Figure 11B). Of note, over 78% of primary DLBCL with high BCL6 and low PTPROt transcript levels were previously identified as "BCR-type" tumors (Figure 11B, Chi-square test, $p < .001$).

4.2. PTPROt is a BCL6 target gene

The reciprocal patterns of BCL6 and PTPROt expression in normal B cells and primary DLBCL and the identification of BCL6-high/PTPROt-low "BCR-type" DLBCL raised the possibility that PTPROt was a target gene of BCL6. To investigate this postulated relationship, a bioinformatic analysis of PTPROt promoter was performed. Specifically, the presence of a structural BCL6-binding motif was sought. The 1.5 kb PTPROt promoter region, which encompassed the previously identified transcription start site (TSS) and TATA box [50, 58], included 3 candidate BCL6 binding sites (–763 to –746; –124 to –107; +300 to +317 nt from TSS). Of note, the two upstream candidate BCL6 binding sites (–763 to –746 and –124 to –107) are located within a region of the PTPROt promoter associated with repressed basal transcriptional activity [58].

To assess the functional status of the candidate BCL6 binding sites, a luciferase vector driven by the PTPROt promoter (pGL3-Luc-PTPROt--1108+381) was generated. This PTPROt-luciferase

construct was cotransfected into HEK293T cells with a vector encoding either wild-type BCL6 or one of two inactive BCL6 mutants, BCL6-ZF or BCL6-ΔZF (lacking the amino-terminal transcriptional repressor domain or carboxy-terminal DNA binding zinc-finger sequence, respectively). WT BCL6 repressed PTPROt-driven luciferase activity in a dose-dependent manner (Figure 12A); in marked contrast, neither of the inactive BCL6 mutants decreased expression of the PTPROt reporter gene (Figure 12B).

To investigate whether endogenous BCL6 binds the PTPROt promoter region *in vivo,* a chromatin immunoprecipitation assay was utilized. In two "BCR-type" DLBCL cell lines (DHL4 and DHL6), DNA fragments including the predicted BCL6 binding sites, but not two upstream/downstream control fragments, were significantly enriched in a-BCL6 chromatin immunoprecipitates (Figure 13A). These data suggest that each of the identified binding sites is occupied by BCL6 *in vivo* (Figure 13A). Consistent with these observations, individual mutations of each of the predicted BCL6 binding sites decreased BCL6-mediated repression of PTPROt and combined mutations of all 3 BCL6 binding sites in PTPROt promoter abolished its response to BCL6 (Figure 13B). Taken together, these results indicate that BCL6 represses the activity of the PTPROt promoter and that this function requires the identified BCL6 binding sites.

4.3. BCL6 regulates PTPROt expression in normal B cells and DLBCL

Given the reciprocal, developmentally regulated pattern of expression of BCL6 and PTPROt in normal B cells, it was of interest whether PTPROt is a physiological target of BCL6 in highly purified naïve B-cells and GC centroblasts. After transducing naïve B cells with a BCL6 lentiviral vector and centroblasts with a BCL6-shRNA construct, PTPROt expression was assessed by RT PCR (Figure 14A). In naïve B cells, the forced overexpression of BCL6 markedly decreased PTPROt transcript abundance (Figure 14A, left panel). Conversely, BCL6 depletion increased PTPROt expression in normal centroblasts (Figure 14A, right panel).

After demonstrating that PTPROt is a physiological target of BCL6 in normal B-cells (Figure 14A), BCL6 role in modulation of PTPROt expression in a representative "BCR"-type DLBCL cell line was assessed (Figure 14B). Under conditions in which BCL6 siRNA increased the abundance of known BCL6 target gene FCER2 (data not shown), BCL6 depletion increased PTPROt transcript abundance 10-fold (Figure 14A). Of note, BCL6 depletion did not change the expression of total SYK, upstream BCR pathway components such as CD79a or downstream adapter proteins such as BLNK. These data indicate that BCL6 specifically modulates PTPROt expression in normal B cells and certain DLBCL.

4.4. BCL6-mediated repression of PTPROt increases SYK Y352 phosphorylation and promotes BCR signaling

After demonstrating that PTPROt is a transcriptional target of BCL6, the consequences of BCL6 depletion on SYK phosphorylation and tonic BCR signaling in a representative "BCR"-type DLBCL cell line (DHL4) were assessed. The DLBCL line was transduced with BCL6-siRNA or scrambled control; thereafter, cells were lysed, immunoprecipitated with pan SYK antibody and immunoblotted with an anti-phospho SYK Y352 antibody. SYK phosphorylation was markedly lower in BCL6-depleted cells than in parental or mock-transduced cells (Figure 15A). Next, single-cell phospho-specific flow cytometry was used to specifically assess SYK Y352 phosphorylation and BCR signaling following BCL6 knockdown. Tonic and BCR crosslink-associated phosphorylation of SYK Y352 was much lower in BCL6-depleted cells than in control and parental cells (Figure 15B). Phosphorylation of the associated adaptor protein, BLNK, was similarly decreased in BCL6-depleted, but not in control or parental cells (Figure 15B). Taken together, these data confirm that BCL6 regulates tonic and BCR-crosslink-induced signaling of the BCR pathway by repressing SYK phosphatase, PTPROt.

Discussion

The molecular characteristics of the "BCR" DLBCL subtype defined by the comprehensive genetic signature suggested that these tumors might be reliant on BCR/SYK signaling pathway and BCL6 transcriptional program. To investigate these hypotheses, a comprehensive genetic, molecular and biochemical studies were performed to specifically assess the role of BCR/SYK-dependent signaling in "BCR"-type DLBCL and the biological consequences of its inhibition *in vitro*, mechanisms controlling SYK activity, role of transcriptional program controlled by BCL6 and the biological consequences of its inhibition *in vitro*, and relationship between BCL6 mediated repression and SYK-dependent signaling in "BCR"-type DLBCL.

Performed studies functionally characterized the molecular signature of "BCR"-type DLBCL

and identified BCR signaling and BCL6 transcriptional program to be critical pro-survival mechanisms in this DLBCL subtype. These findings have direct translational consequences, since both pathways are therapeutically targetable. In addition, a novel mechanism controlling BCR activity via BCL6 mediated repression of PTPROt was identified, demonstrating that both pathways are functionally related and suggesting that a combined inhibition could have synergistic effect in these DLBCL.

1. Characterization of critical survival role of tonic SYK-dependent BCR signaling in "BCR" type DLBCL

The majority of examined DLBCL cell lines exhibit tonic BCR signaling as evidenced by basal phosphorylation of SYK348 and 352 and the SYK-dependent linker protein, BLNK. DLBCL cell lines with an intact BCR signaling pathway were highly sensitive to the ATP-competitive SYK inhibitor, R406, which blocked downstream signaling and induced apoptosis. Of interest, the DLBCL cell lines with an intact BCR signaling pathway and sensitivity to the SYK inhibitor were independently identified as "BCR" tumors on the basis of their transcriptional profiles. These data suggest that tonic BCR signaling is an important and potentially targetable survival pathway in these DLBCL and that R406-sensitive DLBCL can be identified by their transcriptional profiles. Of importance, tonic and induced BCR signaling and R406 responses are detectable in some, but not all, primary DLBCL, indicating that the findings in DLBCL cell lines are directly applicable to primary tumors and highlighting the potential value of profile-defined comprehensive clusters [9] with targetable subtype-specific survival pathways. For all of these reasons, SYK is an attractive rational target in DLBCL and possibly other B-cell malignancies and R406 is a promising targeted treatment. Safety and efficacy of the oral, single daily dose of R406 (FosD) in patients with relapsed/refractory DLBCL (and other lymphoid malignancies) was evaluated in a recently completed phase I/II clinical trial [59]. FosD was very well tolerated and exhibited encouraging efficacy in these patients. Response rate in relapsed refractory DLBCL patients was 21%, 54% in small lymphocytic/chronic lymphocytic leukemia (SLL/CLL), 10% in follicular lymphoma (FL), and 11% in mantle cell lymphoma (MCL) [59]. Stable disease was observed in an additional 23 patients, including 12 with FL, 4 with DLBCL, 4 with MCL, 2 with CLL/SLL and 1 with mucosa-associated lymphoid tissue lymphoma [59]. Given the heavily pretreated cohort of patients enrolled in this study and encouraging results of FosD used as a single oral agent, it can be expected that clinical applications of FosD will be further developed, especially in rational combinations for BCR-dependent B-cell non-Hodgkin lymphoma (NHL).

2. Mechanisms and regulation of tonic BCR signaling in "BCR" tumors

Given the critical role of tonic BCR signaling in normal B-cell development and lymphomagenesis, it could be expected that this process remains under tight control. Tonic BCR signaling is thought to be initiated and regulated by stochastic interactions between PTKs and PTPs within cell membrane lipid rafts. In this homeostatic equilibrium model [14], positive regulators transiently and stochastically interact with the BCR complex and activate receptor-associated PTKs, ITAM phosphorylation, assembly of Ig/signaling complexes, and SYK phosphorylation. This positive PTK-associated regulatory arm is counterbalanced by the recruitment of negative regulators such as PTPROt. Inhibition of the PTP-dependent negative-regulatory arm stabilizes and enhances tonic BCR signals. The role of PTPs in regulating tonic BCR signaling was first suggested by studies in which BCR-proximal PTKs were activated by treatment with the phosphatase inhibitor, pervanadate/H_2O_2, in the absence of BCR cross-linking [14, 15, 19, 20]. The current study identifies PTPROt as a critical mechanism for enhanced SYK-dependent tonic BCR signaling.

PTPROt is a tissue-specific PTP that is expressed and developmentally regulated in B lymphocytes. PTPROt is a member of the PTPRO family (also designated GLEPP, PTP-ϕ, PTP-OC and PTPu2), a group of highly conserved receptor-type PTPs with a single catalytic domain and transmembrane region and a variably sized extracellular sequence [60, 61]. PTPRO includes an extended extracellular domain whereas PTPROt contains a truncated extracellular region. Initial studies suggested that PTPROt is developmentally regulated and decreased in abundance in normal germinal center B cells and a subset of B-cell lymphomas [50]. In previous studies, PTPROt overexpression markedly increased G0/G1 arrest, providing the first evidence that this PTP regulated B-cell growth [50]. In the current study, the overexpression of PTPROt inhibited BCR-triggered SYK tyrosyl phosphorylation, activation of associated adaptor proteins, and downstream signaling events including MAPK/ERK activation, and cellular proliferation. Of interest, the overexpres-

sion of PTPROt also inhibits lymphoma-cell proliferation and induces apoptosis in the absence of BCR cross-linking, suggesting that PTPROt modulates tonic BCR signaling. The functional consequences of PTPROt overexpression, including decreased SYK phosphorylation, BCR signaling, and cellular proliferation, highlight its likely role in quiescent naive and memory B cells. These observations are of additional interest as SYK is required for B-cell maturation, follicle entry, and recirculation [40, 62–64].

3. BCL6 transcriptional program in "BCR"-type DLBCL

Increased expression and more common translocations of BCL6 in "BCR" tumors suggested that these tumors would exhibit differential regulation of BCL6 target genes that would identify tumors specifically driven by BCL6 and sensitive to BPI treatment. For these reasons, a ChIP-on-chip approach was utilized to identify BCL6 target genes in an aggressive B-cell lymphoma cell line and assess their expression and biological function in "BCR" tumors. The BCL6 target gene list was enriched in genes regulating transcription, DNA damage responses, chromatin modification, cell cycle and protein ubiquitylation (Table 1). Since the mechanism(s) through which BCL6 mediates the germinal center reaction and lymphomagenesis are largely unknown, these data provide new insights regarding BCL6 function in these processes. In more recent studies, BCL6 was shown to regulate similar functionally coherent set of pathways involved in DNA repair, cell cycle, chromatin formation and regulation, protein stability and transcriptional regulation in both normal GC cells and in DLBCL [65]. However, deregulation of BCL6 in DLBCL results in gain of many target genes, implying an expansion of the BCL6 function in lymphoma cells compared to their normal counterparts [65].

BCL6 target genes were coordinately repressed in "BCR" tumors, indicating that the BCL6 signature contributes to the difference between "BCR" and other molecular tumor classes that are not BCL6-dependent. In addition, BPI treatment increased the expression of each of these BCL6 targets in the "BCR" DLBCL cell lines but did not alter the expression of these genes in other tumor types. These data suggest that BCL6 is biologically active in "BCR", but not in "non-BCR", tumors and show that BCL6 represses its target genes in "BCR" DLBCL regardless of their baseline levels. Finally, the "BCR" consensus cluster designation was more accurate in predicting BPI sensitivity than either BCL6 protein expression alone or the absolute levels of BCL6 target genes.

Taken together, this approach, combining stringent genomic localization by ChIP on chip with large-scale functional genomics and the use of a specific transcription factor inhibitor highlights the important contribution of an oncogenic transcription factor to the transcriptional programming of a human tumor. From a clinical standpoint, these data indicate that patients with "BCR" DLBCL may represent the best candidates for therapeutic trials of BCL6 inhibitors. Standard diagnostic methods will not delineate these patients. Development of methods to identify tumors most likely to respond to targeted therapy is an important advance since it allows for molecular stratification of patients to therapeutic arms. More broadly, these data show how integration of genome-wide transcription factor binding and gene expression profiling can provide important insights into tumor biology, identify the presence of gene regulatory programming by oncogenic transcription factors, and direct selection of tumors for targeted therapeutic agents.

4. Characterization of BCL6 role in promoting BCR signaling

Since the same transcriptionally defined subset of DLBCL relies upon SYK-dependent BCR signaling and exhibits coordinate BCL6-mediated transcriptional repression, the relationship between these two processes was explored. These studies demonstrated that in normal GC B cells, PTPROt is repressed by BCL6. The finding that BCL6 suppresses PTPROt identifies a novel function for BCL6 in normal GC B cells. Within the GC, centroblasts proliferate rapidly and undergo somatic hypermutation of their immunoglobulin genes, which is the basis for affinity-maturation of antibodies [4, 22]. BCL6-mediated repression of the SYK phosphatase, PTPROt, likely lowers the threshold for tonic and ligand-induced signals from low-affinity BCRs in GC B cells, facilitating their survival. Once high-affinity BCRs are generated, enhanced ligand-induced BCR signaling promotes BCL6 downregulation via MAPK-dependent phosphorylation of BCL6 PEST domains and associated proteasomal degradation, licensing exit from the GC [39].

The tight spatio-temporal control of BCR signaling by BCL6 is likely altered in DLBCL with deregulated BCL6 expression. In DLBCL with the constitutive expression of BCL6, repression of PTPROt augments SYK-dependent BCR signaling. These observations identify a novel BCL6-dependent pro-survival pathway in B-cell lymphomage-

nesis. Since BCL6 and SYK are both promising rational therapeutic targets in the same group of DLBCL, combined inhibition of these functionally related pathways warrants further study.

Conclusions

1. Molecular signature of the "BCR" type DLBCL has biological and functional background in the constitutive activity of the BCR pathway. Tonic SYK-dependent signaling is a critical survival pathway in these DLBCL and can be therapeutically targeted with a specific ATP-competitive inhibitor of SYK (R406),
2. SYK activity is physiologically controlled by a tissue-specific and developmentally regulated protein tyrosine phosphatase (PTPROt). Overexpression of the phosphatase blocks proximal BCR signaling and downstream events and induces cell apoptosis,
3. "BCR"-type DLBCL exhibit coordinate regulation of the identified BCL6 target genes. BCL6 signature and "BCR" subtype designation have important functional consequences because disruption of the BCL6 transcriptional program with peptide-mediated interference specifically inhibits growth of "BCR"-type cell lines,
4. BCR signaling and BCL6-mediated transcriptional repression are functionally related in "BCR"-type DLBCL. In this tumor subtype, the constitutive expression of BCL6 represses PTPROt and augments SYK-dependent BCR signaling. These observations identify a novel BCL6-dependent pro-survival pathway in B-cell lymphomagenesis and highlight the possible synergism of combined inhibition of these functionally related pathways.

Acknowledgements

I would like to thank all collaborating investigators: Ricardo C.T. Aguiar, Linfeng Chen, Wen Chen, Leandro Cerchietti, John Daley, Riccardo Dalla-Favera, John M. Greally, Thomas A. Habermann, Jeffery Kutok, Ari Melnick, Stefano Monti, Evan O'Donnell, Jose M. Polo, Stella M. Ranuncolo, Kunihiko Takeyama, Thomas E. Witzig, Kenny Ye.

Special thanks for my mentor and advisor, Margaret Shipp.

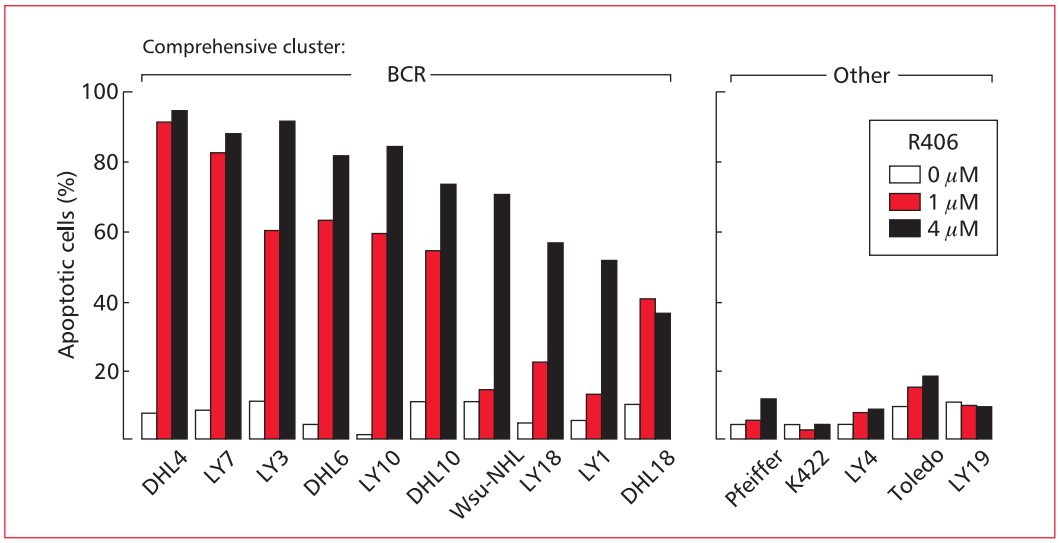

Figure 1. The SYK inhibitor, R406, induces apoptosis in a subset of DLBCL cell lines. DLBCL cell lines were cultured with 1 mM or 4 mM of R406 or vehicle alone for 96 hours. Thereafter, cellular apoptosis was assessed using annexin V–FITC/propidium iodide (PI) staining. All of the R406-sensitive cell lines (left panel) were previously designated as "BCR-type" DLBCL using the cell line transcriptional profiles and a recently described ensemble comprehensive cluster classifier [34]. None of the R406-insensitive cell lines were identified as "BCR-type" ("Other", right panel)

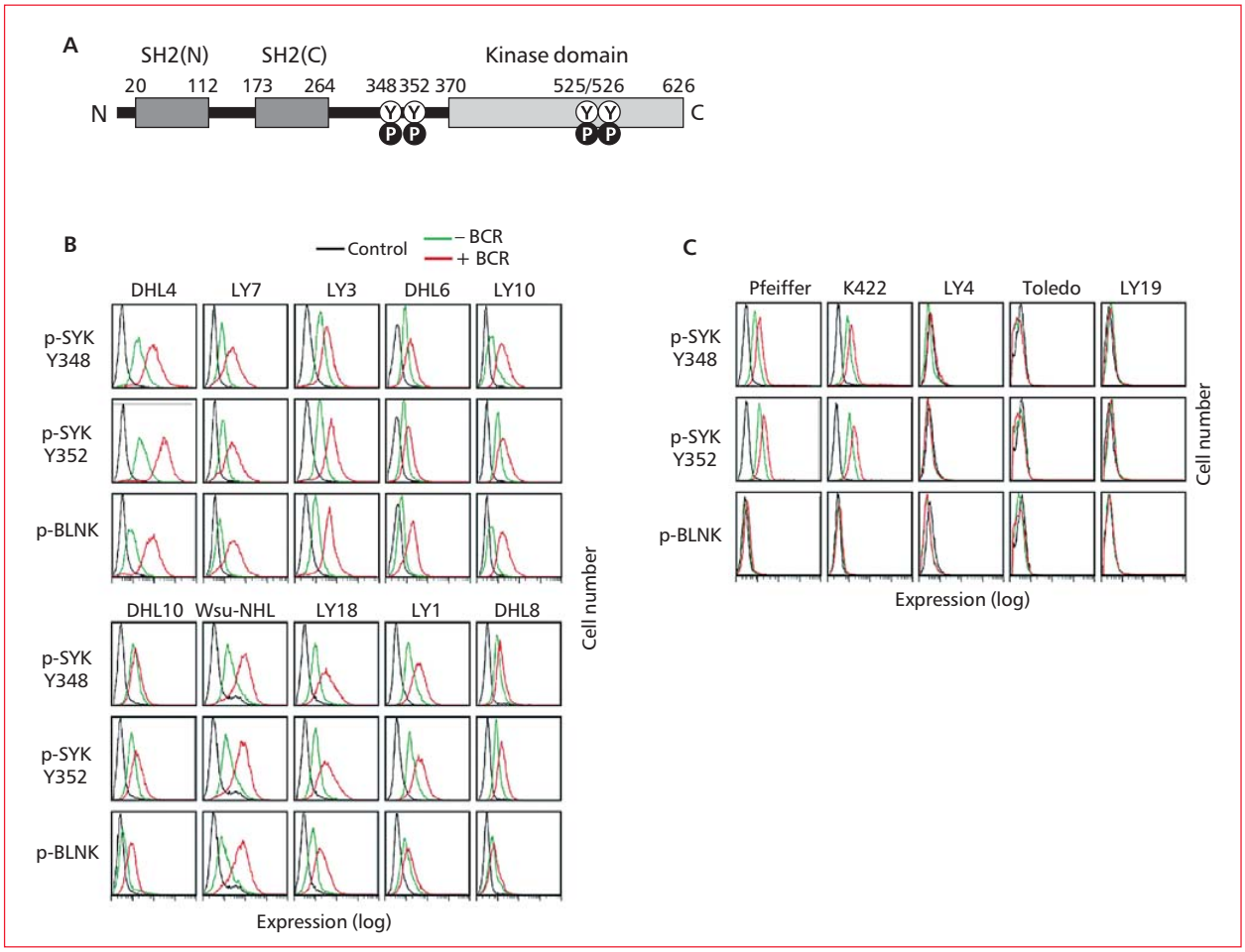

Figure 2. BCR signaling is intact in R406-sensitive DLBCL cell lines. (A) SYK domains and key tyrosine residues. The SYK tandem SH2 domains (black boxes), the linker region (aa 264-370), and the kinase domain (gray box) are shown. N indicates NH2-terminal; C, C-terminal; Y, tyrosine; P, phosphorylation. Following BCR engagement, LYN induces phosphorylation of SYKTyr348 and Tyr352 in the linker region. Thereafter, SYK undergoes autophosphorylation of SYKTyr525/526 and associated activation. (B). Tonic BCR signaling in R406-sensitive and -resistant DLBCL cell lines. Single-cell phospho-specific flow cytometry was used to assess low-level SYK348 and 352 and BLNK phosphorylation in the absence (green) or presence (red) of BCR crosslinking (10 min) in R406-sensitive (B) and -resistant (C) DLBCL cell lines. Cells stained with an isotype-matched control Ig are shown in black. The x-axis denotes expression (log scale) and the y-axis indicates cell number

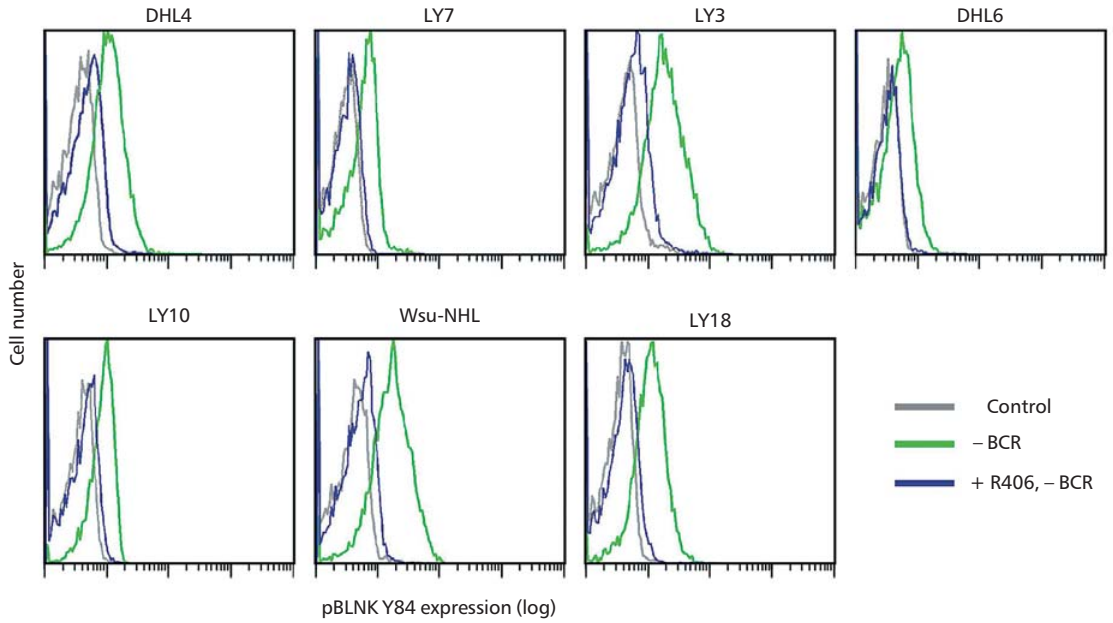

Figure 3. R406 inhibits tonic BLNK tyrosine phosphorylation in DLBCL cell lines. DLBCL cell lines were treated with 4 mM of R406 (blue) or vehicle alone (green) at 37°C for 16 hours without crosslinking the BCR receptor (-BCR). Tonic BLNK phosphorylation in R406- or vehicle- treated cells was detected by single-cell phospho-flow cytometry. Gray lines represent cells stained with an isotype-matched control Ig

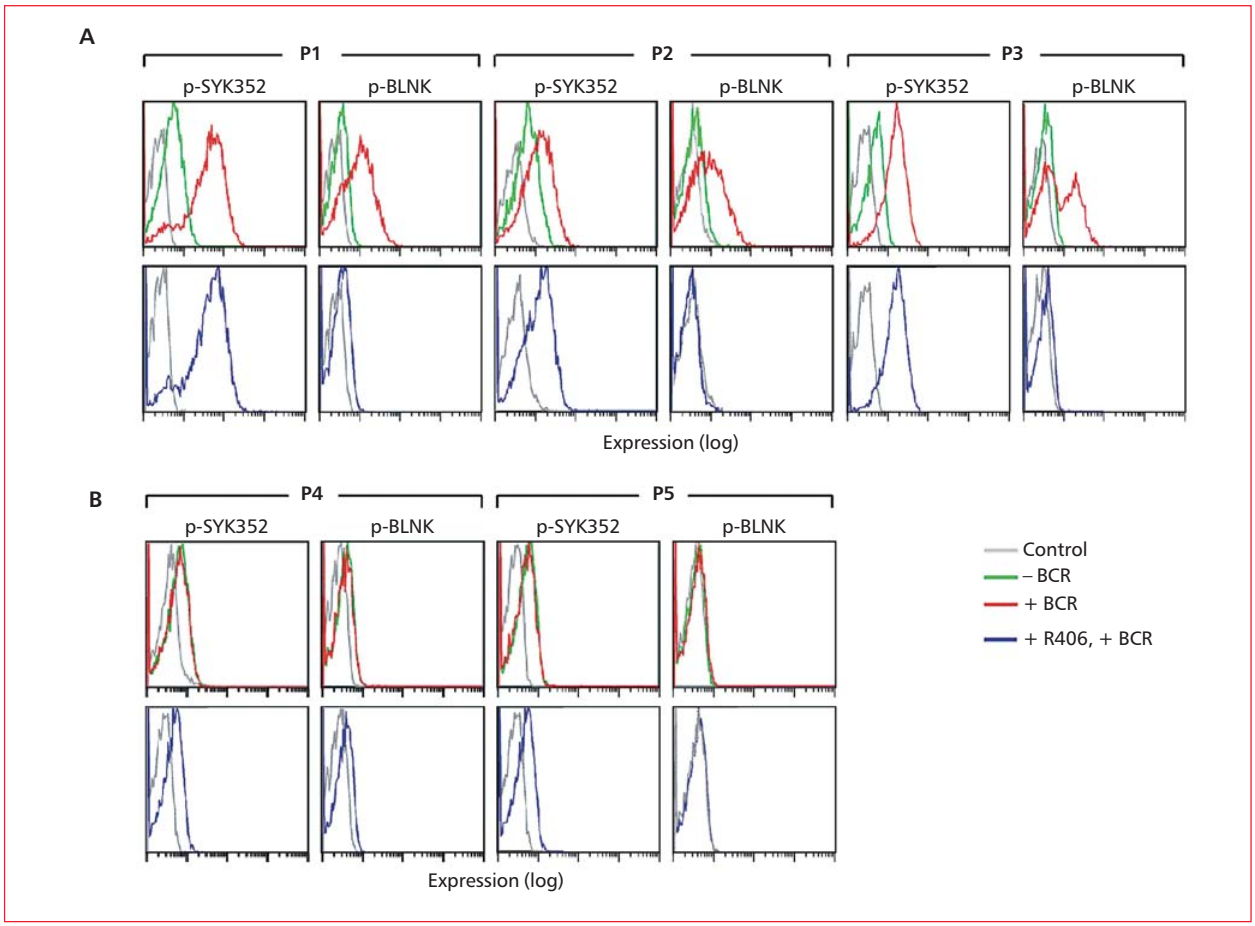

Figure 4. BCR signaling in primary DLBCL. Cryopreserved tumor cell suspensions were thawed and viable tumor cells were isolated from a Ficoll Hypaque monolayer. Thereafter, the tumor cell suspensions were over 90% viable by Trypan blue staining. Light microscopy, light scatter analysis at flow cytometry, and cell-surface Ig expression confirmed the presence of a predominant population of tumor cells. (**A**,**B**) BCR signaling in primary DLBCL. Single--cell phospho-flow cytometry was used to assess pSYK352 and pBLNK expression in the absence (green) or presence (red) of BCR crosslinking or BCR crosslinking following R406 treatment (blue). Primary DLBCL with intact BCR signaling (**A**) and ineffective BCR signaling (**B**) are shown. Cells stained with isotype-matched control Ig are shown in gray

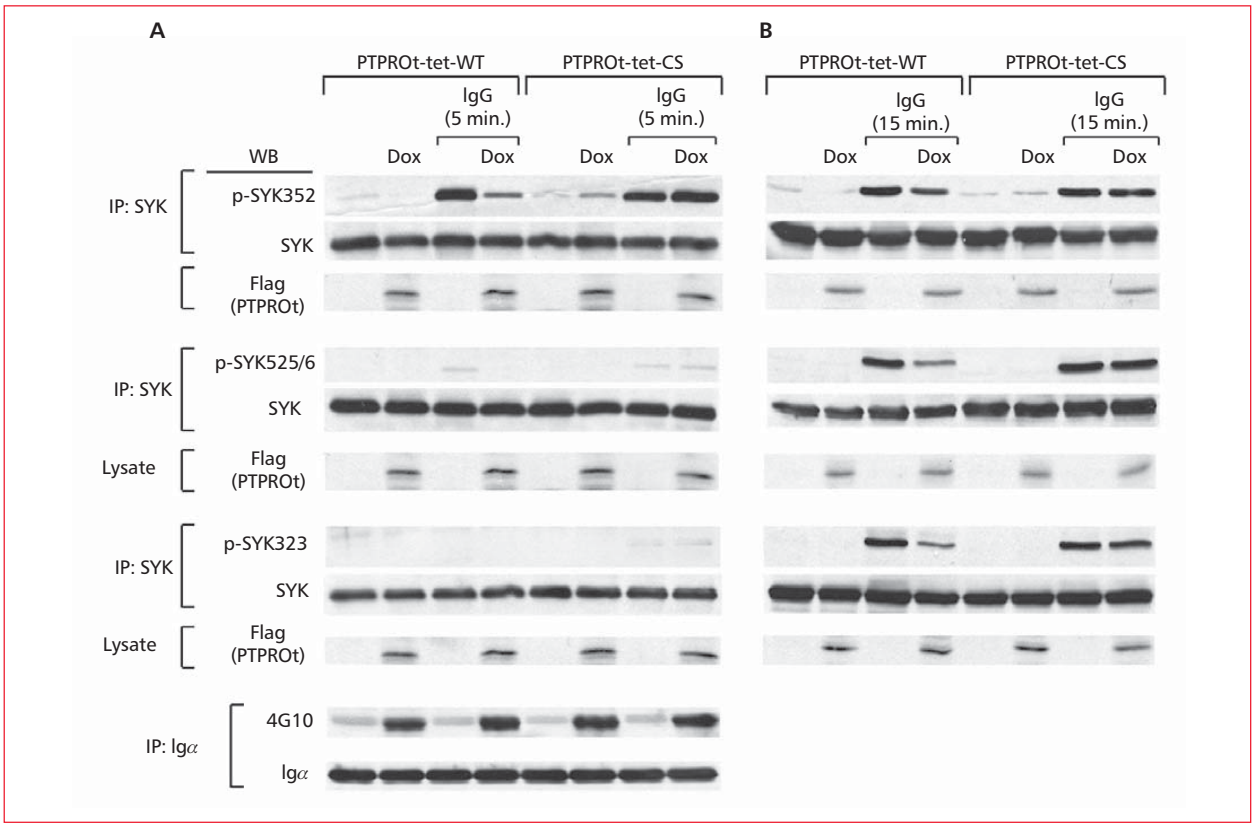

Figure 5. PTPROt inhibits SYK tyrosyl Y352 phosphorylation. Tet-inducible FLAG-tagged WT or mutant (CS) PTPROt clones were cultured with or without Dox and stimulated with goat anti–human IgG for 5 (A), 15 (B) minutes, or left untreated. Thereafter, cells were lysed and immunoprecipitated with anti-SYK or anti-CD79a antibody. Immunoprecipitates were size fractionated, blotted, and analyzed with indicated phosphotyrosine antibodies (a pSYK352, pSYK525/526, pSYK323, 4G10). The blots was subsequently stripped and blotted with an anti-pan SYK or anti-CD79a antibody. In each experiment, the corresponding whole cell lysates were simultaneously size-fractionated, blotted, and analyzed with FLAG antibody to confirm Dox-induced overexpression of WT-PTPROt or CS-PTPROt

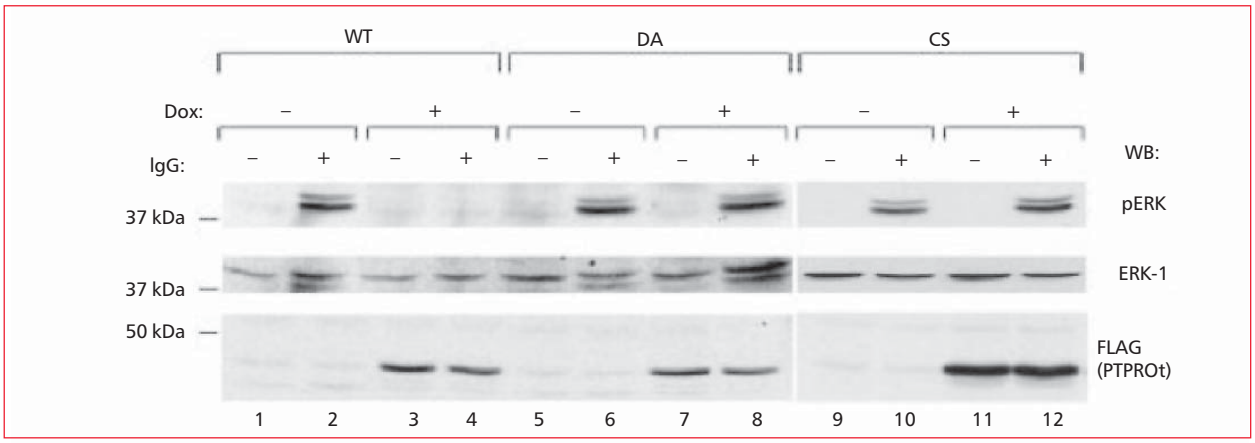

Figure 6. PTPROt inhibits ERK phosphorylation. Tet-inducible FLAG-tagged WT or mutant (DA and CS) PTPROt clones were cultured with or without Dox, serum starved, and stimulated with goat anti–human IgG (10 μg/mL) for 8 minutes or left untreated. Thereafter, total cell lysates were size fractionated, blotted, and analyzed with anti--phospho-ERK1/2 antibody (top panel). The blot was then stripped and reprobed with anti-ERK1 (middle panel) and anti-FLAG antibodies (bottom panel)

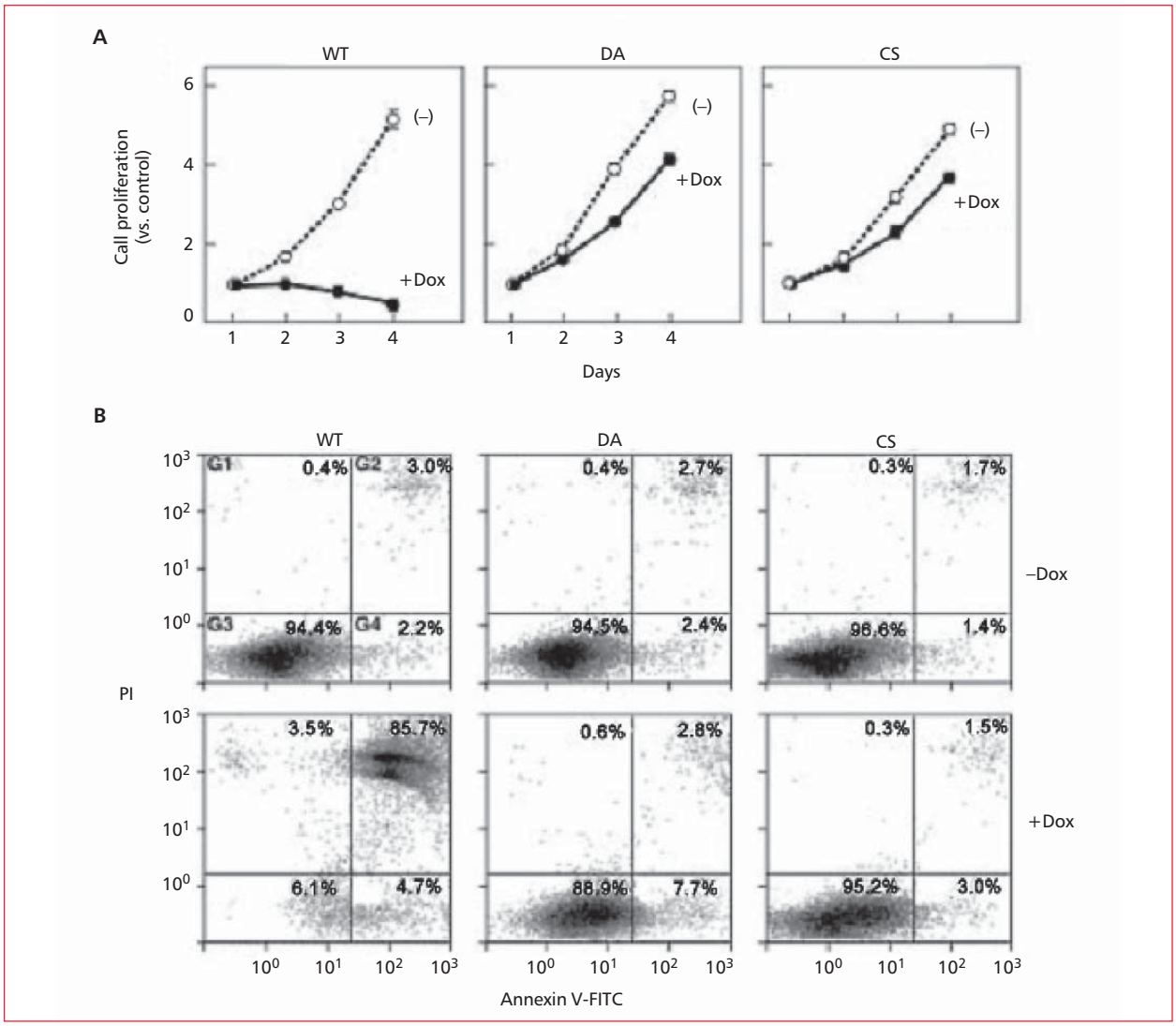

Figure 7. PTPROt overexpression inhibits cellular proliferation and induces apoptosis. (A) Cellular proliferation of tet-inducible PTPROt clones. Tet-inducible FLAG-tagged WT, CS, or DA PTPROt clones were cultured with or without Dox for 1 to 4 days (x-axis) and analyzed in MTT proliferation assays. Proliferation on days 2 to 4 is represented as fold increases compared with the initial day-1 measurement (y-axis). (B) Apoptosis of tet-inducible PTPROt clones. Tet-inducible FLAG-tagged WT, CS, or DA PTPROt clones were cultured with or without Dox for 4 days and analyzed thereafter with annexin V–FITC/PI staining. (x- and y-axes, respectively). The percentages of cells staining with PI alone (G1), annexin V and PI (G2), annexin V alone (G4), or neither reagent (G3) are indicated

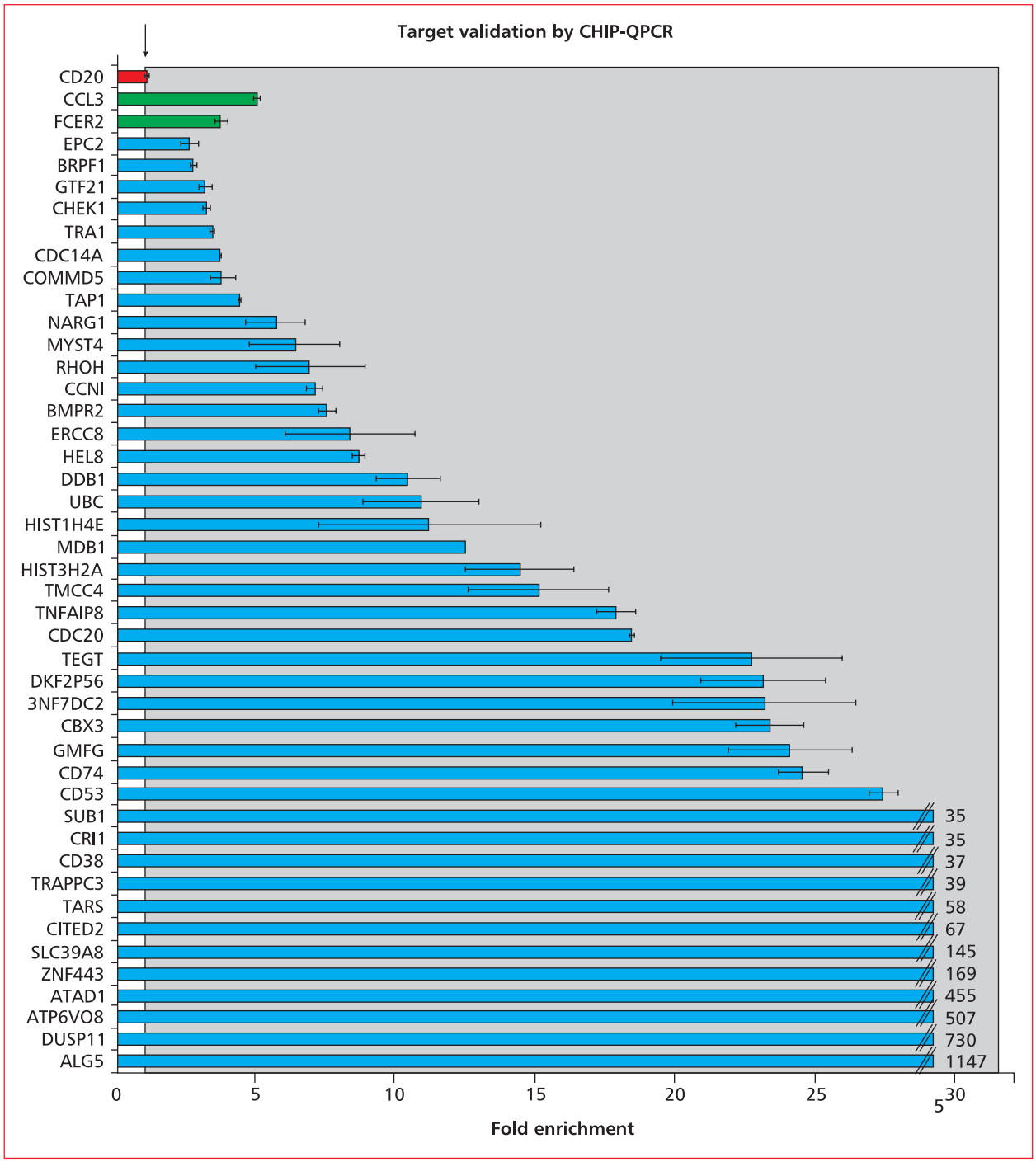

Figure 8. Validation of candidate BCL6 target genes by quantitative ChIP assay. Forty-four (out of 54 tested) candidate BCL6 target genes were validated. The X axis represents the fold enrichment for each promoter region *vs.* IgG control antibody after normalization to input DNA. The target gene amplicons represent the enriched regions based on the localization of the BCL6 peak on the ChIP on chip array. *CCL3* and *FCER2* are known BCL6 target genes that were enriched by ChIP on chip and are included as positive controls (green); *CD20* is included as negative control (fold enrichment = 1, red)

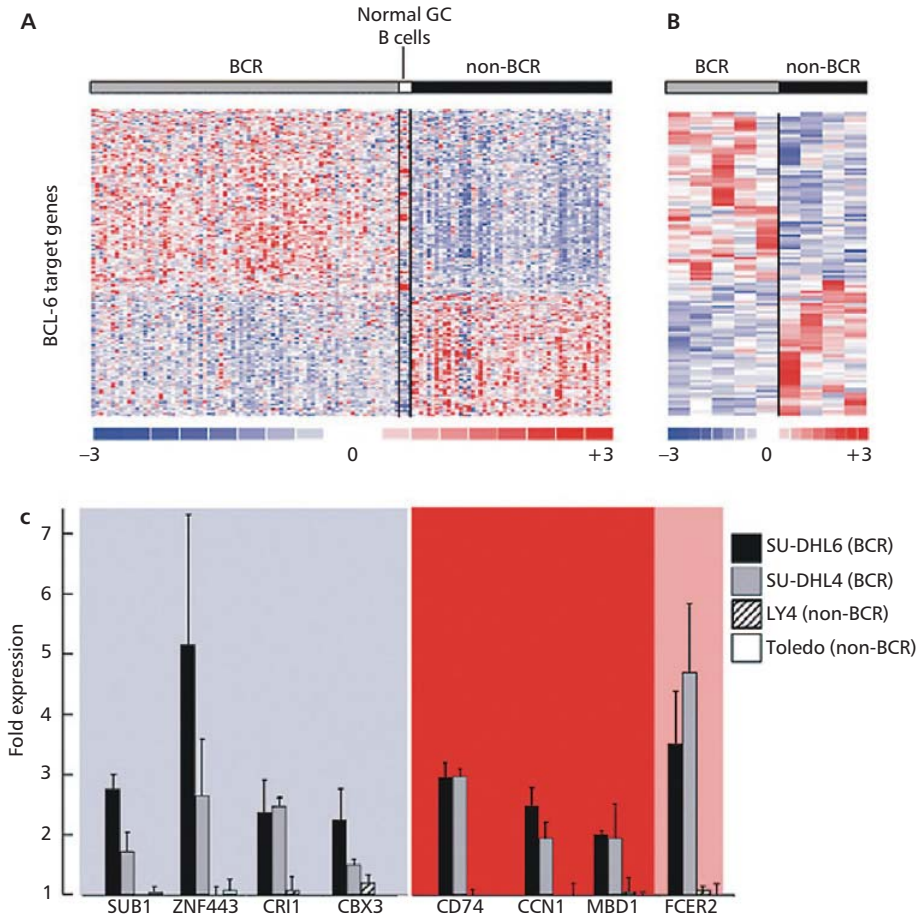

Figure 9. BCL6 target genes in primary "BCR" and "non-BCR" DLBCL and DLBCL cell lines. The top-scoring BCL6 target genes from the GSEA leading edge were clustered with respect to the DLBCL "BCR" and "non-BCR" phenotypes and represented on a heat map in which each individual column represents a tumor and each individual row corresponds to a gene. For comparison, the relative expression of these BCL6 target genes in normal GC B-cells is also shown. Color scale at bottom indicates relative expression and standard deviations from the mean. (A) Primary DLBCL heat map [9]. (B) DLBCL cell line heat map ("BCR" cells: Ly1, Ly7, SU-DHL4, SU-DHL6 and Farage; "non-BCR" cells: Ly 4, Toledo, Kaspas 422 and Pfeiffer). (C) BCL6 target gene abundance in "BCR" and "non-BCR" cell lines following BPI treatment. "BCR" (SU-DHL6, SU-DHL4) and "non-BCR" (Toledo, Ly4) cell lines were treated with 20 mM of BPI or control peptide for 8 hours and the transcript abundance of the indicated BCL6 targets was evaluated with real–time (RT) PCR thereafter. The Y axis indicates fold activation of genes after treatment with BPI *vs.* control peptide based on the $\Delta\Delta^{Ct}$ normalized to the expression of *HPRT*. BPI treatment increased the expression of each BCL6 target gene in the "BCR" cell lines but did not alter the expression of these genes in "non-BCR" lines. BPI treatment increased the abundance of BCL6 targets that were less abundant in "BCR" than "non-BCR" cells at baseline (SuB1, ZNF443, CR1, CBX3, shaded in blue) and others that were more abundant in "BCR" tumors at baseline (CD74, CCN1, MBD1, shaded in red). A known BCL6 target gene FCER2 was used as a positive control (shaded in pink)

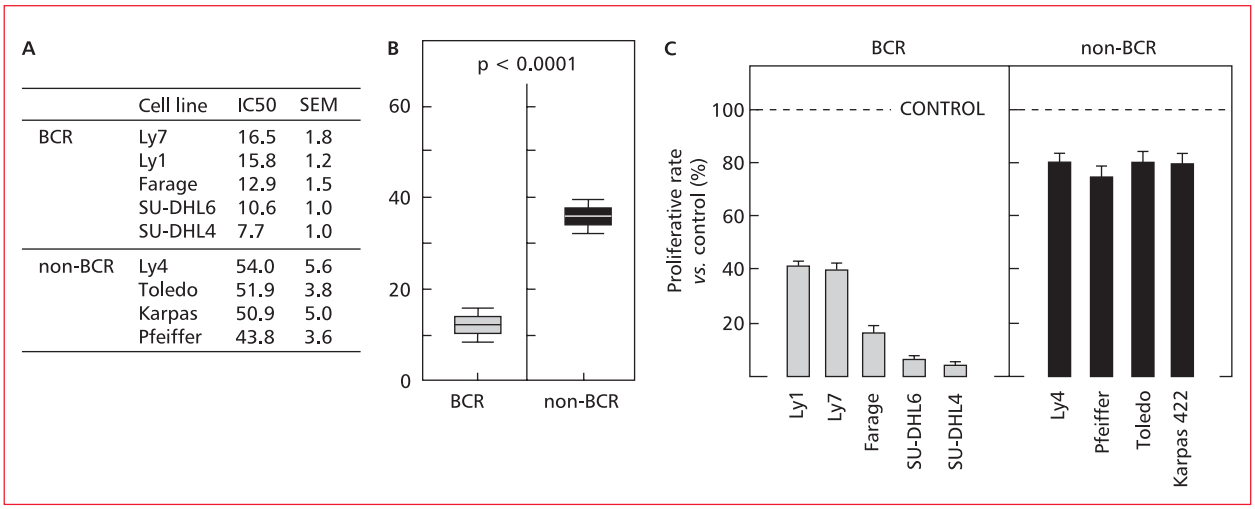

Figure 10. "BCR" and "non-BCR" DLBCL cell lines display differential sensitivity to BPI. (A) BPI IC50 for "BCR" and "non-BCR" DLBCL cell lines. "BCR" and "non-BCR" cell lines were exposed to increasing doses of BPI and cellular proliferation was assessed at 48 hours. The IC50 and SEM for triplicate samples of each cell line in a representative experiment are shown. (B) Mean BPI IC50 (± SD) for "BCR" and "non-BCR" DLBCL cell lines. (C) Proliferation of BPI--treated "BCR" and "non-BCR" DLBCL cell lines following BPI treatment. Cell lines were exposed to 20 mM BPI for 48 hours and cellular proliferation was evaluated thereafter

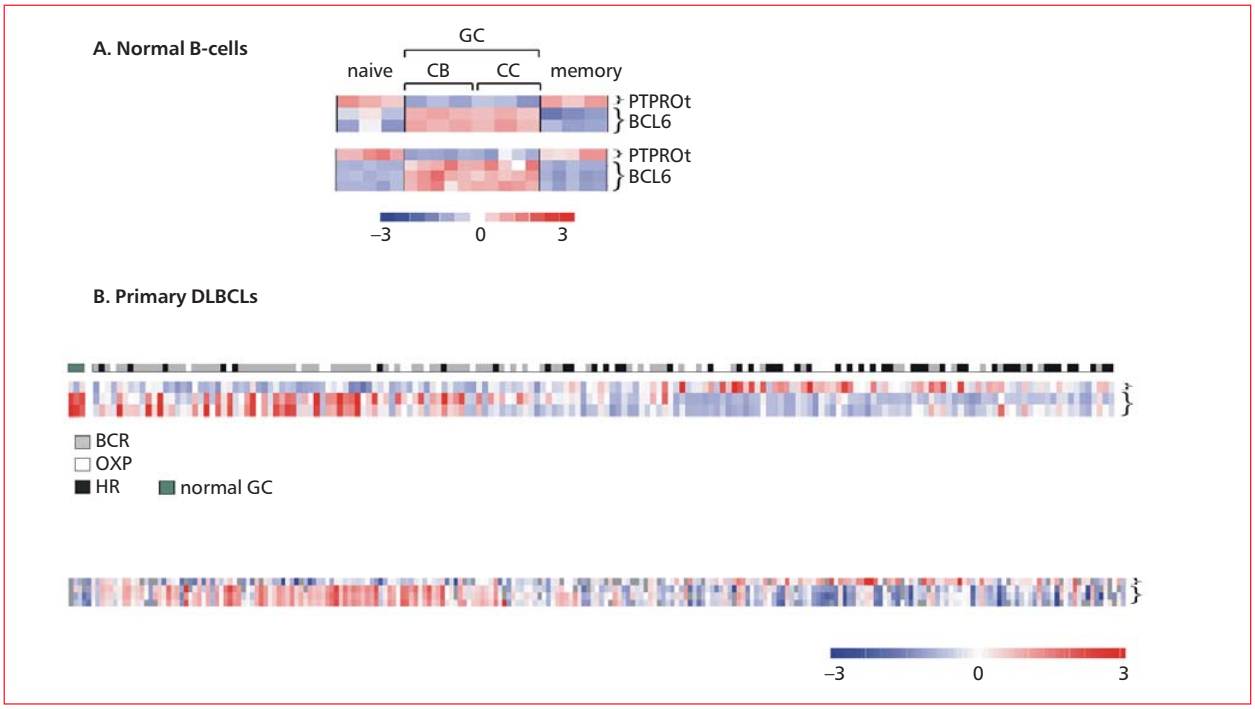

Figure 11. Reciprocal patterns of PTPROt and BCL6 expression in normal B cells and primary DLBCL. (A) Relative BCL6 and PTPROt transcript abundance in two independent series of highly purified normal B-cells (naïve, GC centroblasts [CB] and centrocytes [CC], memory). (B) Relative BCL6 and PTPROt transcript abundance in two large independent series of newly diagnosed and previously profiled DLBCL [9, 10]. Normal GC B cells that were profiled at the same time [9] were included for comparison (left). Comprehensive cluster designations ("BCR", "OxP" and "HR") for the primary DLBCL and normal GC cells in Monti series are indicated above the heat map. Color scale at bottom indicates relative expression and standard deviations from the mean. Red connotes high-level expression; blue indicates low-level expression

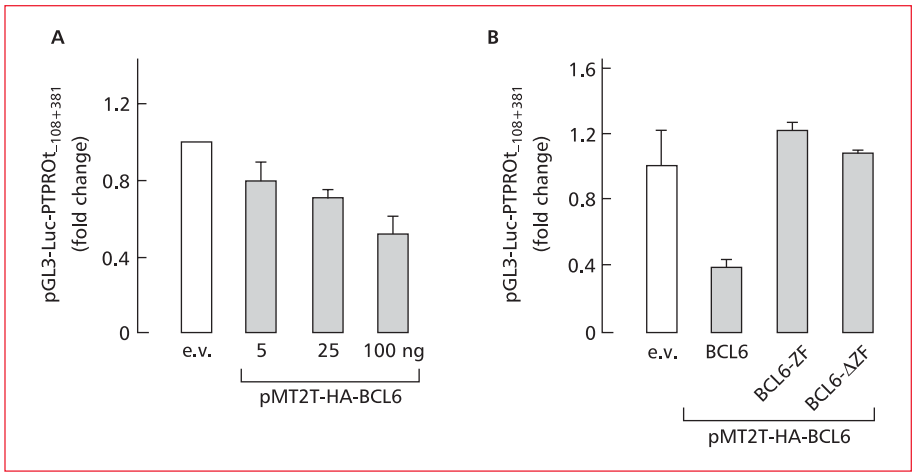

Figure 12. PTPROt transcription is regulated by BCL6. (A) BCL6 represses PTPROt promoter-driven transcription in a dose-dependent manner. A PTPROt promoter luciferase reporter construct (pGL3-Luc-PTPROt-1108+381) was cotransfected with empty vector or increasing does (5–100 ng) of a BCL6 expression vector (pMT2T-HA-BCL6) into HEK293T cells. Luciferase activities were evaluated as described (Methods). (B) WT-BCL6 but not BCL6 mutants repress PTPROt promoter-driven transcription. pGL3-Luc-PTPROt-1103+381 was cotransfected with vectors encoding either HA-BCL6 or one of two BCL6 mutants lacking either the amino-terminal transcriptional repressor domain (BCL6-ZF) or carboxy-terminal DNA binding zinc-finger domain (BCL6-ΔZF) and luciferase activities were determined thereafter. In both A and B, representative luciferase activities from three independent experiments were normalized to Renilla luciferase activity and represented as fold change ± standard deviation

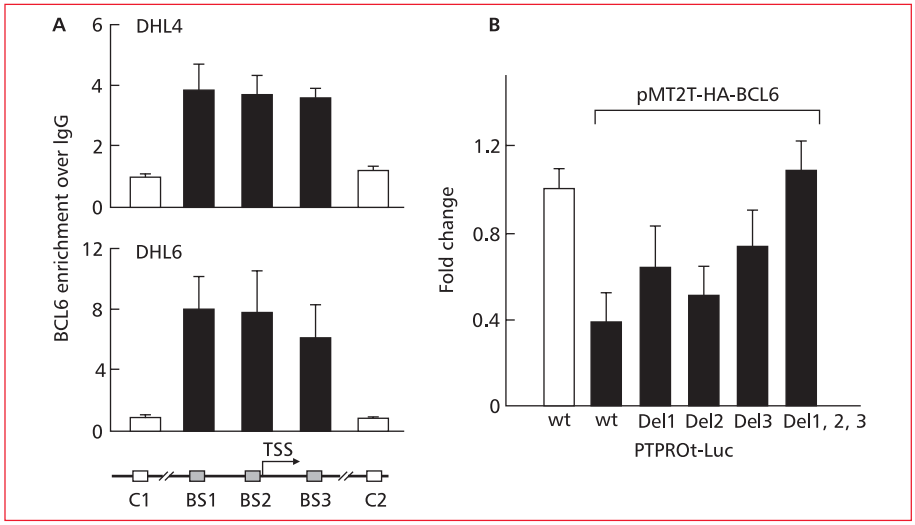

Figure 13. BCL6 represses PTPROt via direct interactions with the PTPROt promoter region. (A) BCL6 binds to the PTPROt promoter *in vivo.* Chromatin immunoprecipitation was performed in two DLBCL cell lines (DHL4 and DHL6) using BCL6 antibody or normal IgG as control. The target amplicons in the PTPROt promoter include the 3 predicted BCL6 binding sites (BS1-3, solid boxes) and two distant upstream or downstream control regions (C1 and C2, open boxes). The BCL6 *vs.* IgG ratio was calculated for each region and normalized to control region 1. (B) BCL6-mediated repression of PTPROt promoter requires intact BCL6 binding sites. PTPROt-promoter-driven luciferase constructs with or without the individual or combined mutations in the predicted BCL6 binding sites were cotransfected with pMT2T-HA-BCL6 into HEK293T cells. Luciferase activities were determined thereafter

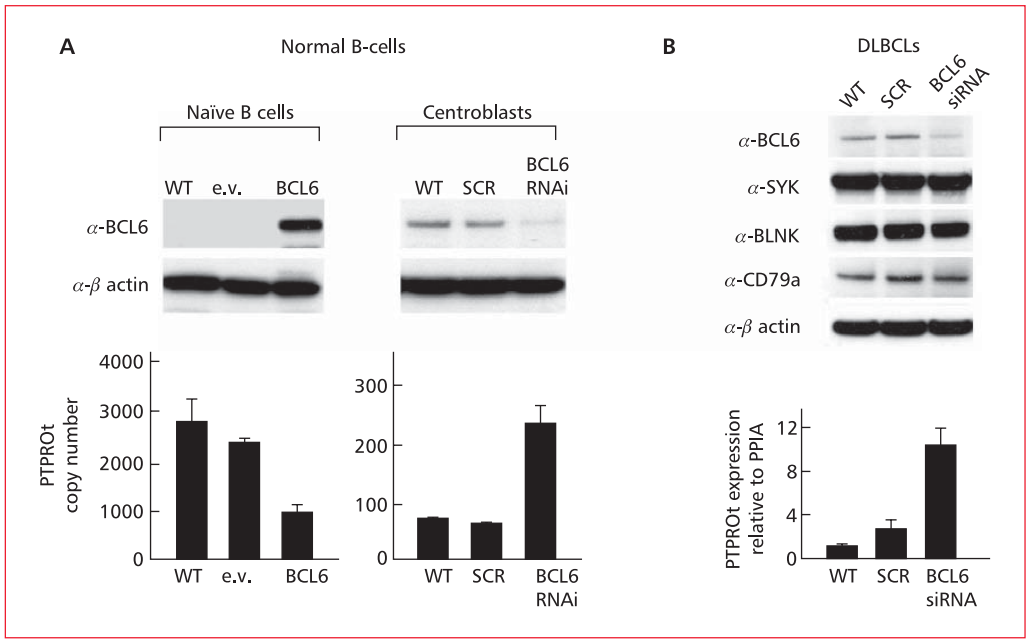

Figure 14. BCL6 regulates PTPROt expression in normal naïve B-cells, GC centroblasts and certain DLBCL. (A) Normal B cells. Normal naïve B-cells were transfected with a GFP-BCL6 construct or empty vector and GC centroblasts were transduced with a BCL6-shRNA lentiviral vector or scrambled control. (B) DLBCL. A DLBCL cell line (DHL4), was transduced with BCL6 siRNA. In both the normal B cells (A) and the DLBCL cell line (B), BCL6 protein levels were assessed by western blot (top panel) and PTPROt expression was evaluated by RT PCR (bottom panel). In DLBCL, expression levels of total SYK, upstream BCR pathway component CD79a and downstream adapter protein BLNK were also evaluated

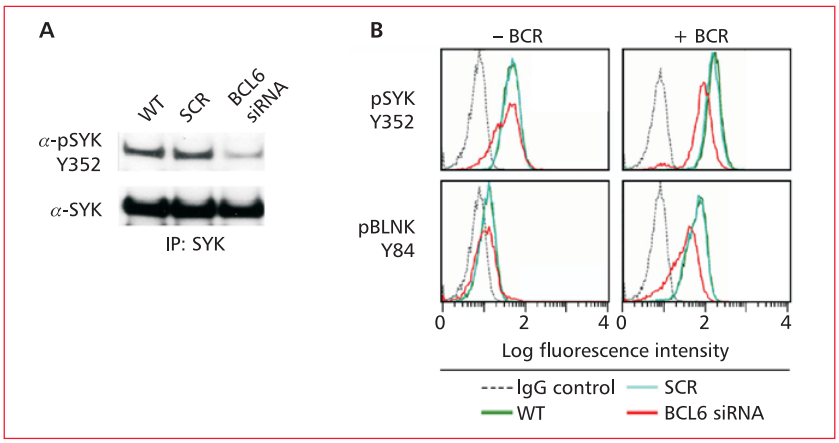

Figure 15. BCL6-mediated repression of PTPROt increases tonic BCR signaling. The DLBCL cell line, DHL4, was transduced with BCL6-siRNA, SCR control oligonucleotides or left untreated. Cells were subsequently incubated for 72 h and stimulated with goat anti–human IgG (10 mg/mL) for 1 minute or left untreated. (A) Western analysis of SYK phosphorylation following BCL6 depletion. BCR-crosslinked cells were lysed and immunoprecipitated with anti- SYK. Immunoprecipitates were size-fractionated, blotted, and analyzed thereafter with a-pSYK Y352 antibody. The membrane was subsequently stripped and blotted with an anti-pan SYK antibody. (B) Phospho-specific flow cytometric analysis of tonic and a-Ig induced SYK Y352 and BLNK Y84 phosphorylation following BCL6 depletion. SYK Y352 and BLNK Y84 phosphorylation (top and bottom panels) was compared in cells transduced with BCL6-siRNA (red), SCR control oligonucleotides (blue) or left untreated (green) in the absence (left panel) or presence (right panel) of BCR crosslinking. Cells stained with an isotype-matched control Ig are also shown (gray dashed line). The x-axis denotes expression (log scale) and the y-axis indicates cell number

References

1. Abramson J.S., Shipp M.A. Advances in the biology and therapy of diffuse large B-cell lymphoma: moving toward a molecularly targeted approach. Blood 2005; 106: 1164–1174.
2. Kuppers R., Klein U., Hansmann M.L., Rajewsky K. Cellular origin of human B-cell lymphomas. N Engl J Med 1999; 341: 1520–1529.
3. Klein U., Goossens T., Fischer M., Kanzler H., Braeuninger A., Rajewsky K., et al. Somatic hypermutation in normal and transformed human B cells. Immunol Rev 1998; 162: 261–280.
4. Klein U., Dalla-Favera R. Germinal centres: role in B-cell physiology and malignancy. Nat Rev Immunol 2008; 8: 22–33.
5. Kramer M.H., Hermans J., Wijburg E., Philippo K., Geelen E., van Krieken J.H., et al. Clinical relevance of BCL2, BCL6, and MYC rearrangements in diffuse large B-cell lymphoma. Blood 1998; 92: 3152–3162.
6. Pasqualucci L., Bhagat G., Jankovic M., Compagno M., Smith P., Muramatsu M., et al. AID is required for germinal center-derived lymphomagenesis. Nat Genet 2008; 40: 108–112.
7. Pasqualucci L., Neumeister P., Goossens T., Nanjangud G., Chaganti R.S., Kuppers R., et al. Hypermutation of multiple proto-oncogenes in B-cell diffuse large-cell lymphomas. Nature 2001; 412: 341–346.
8. A predictive model for aggressive non-Hodgkin's lymphoma. The International Non-Hodgkin's Lymphoma Prognostic Factors Project. N Engl J Med 1993; 329: 987–994.
9. Monti S., Savage K.J., Kutok J.L., Feuerhake F., Kurtin P., Mihm M., et al. Molecular profiling of diffuse large B-cell lymphoma identifies robust subtypes including one characterized by host inflammatory response. Blood 2005; 105: 1851–1861.
10. Rosenwald A., Wright G., Chan W.C., Connors J.M., Campo E., Fisher R.I., et al. The use of molecular profiling to predict survival after chemotherapy for diffuse large-B-cell lymphoma. N Engl J Med 2002; 346: 1937–1947.
11. Wright G., Tan B., Rosenwald A., Hurt E.H., Wiestner A., Staudt L.M. A gene expression-based method to diagnose clinically distinct subgroups of diffuse large B cell lymphoma. Proc Natl Acad Sci U S A 2003; 100: 9991–9996.
12. Takahashi H., Feuerhake F., Kutok J.L., Monti S., Dal Cin P., Neuberg D., et al. FAS death domain deletions and cellular FADD-like interleukin 1beta converting enzyme inhibitory protein (long) overexpression: alternative mechanisms for deregulating the extrinsic apoptotic pathway in diffuse large B-cell lymphoma subtypes. Clin Cancer Res 2006; 12: 3265–3271.
13. Gauld S.B., Dal Porto J.M., Cambier J.C. B cell antigen receptor signaling: roles in cell development and disease. Science 2002; 296: 1641–1642.
14. Monroe J.G. ITAM-mediated tonic signalling through pre-BCR and BCR complexes. Nat Rev Immunol 2006; 6: 283–294.
15. Rolli V., Gallwitz M., Wossning T., Flemming A., Schamel W.W., Zurn C., et al. Amplification of B cell antigen receptor signaling by a Syk/ITAM positive feedback loop. Mol Cell 2002; 10: 1057–1069.
16. Kulathu Y., Hobeika E., Turchinovich G., Reth M. The kinase Syk as an adaptor controlling sustained calcium signalling and B-cell development. EMBO J 2008; 27: 1333–1344.
17. Kraus M., Alimzhanov M.B., Rajewsky N., Rajewsky K. Survival of resting mature B lymphocytes depends on BCR signaling via the Igalpha/beta heterodimer. Cell 2004; 117: 787–800.
18. Lam K.P., Kuhn R., Rajewsky K. In vivo ablation of surface immunoglobulin on mature B cells by inducible gene targeting results in rapid cell death. Cell 1997; 90: 1073–1083.
19. Smith S.H., Reth M. Perspectives on the nature of BCR-mediated survival signals. Mol Cell 2004; 14: 696–697.
20. Wienands J., Larbolette O., Reth M. Evidence for a preformed transducer complex organized by the B cell antigen receptor. Proc Natl Acad Sci U S A 1996; 93: 7865–7870.
21. Kuppers R. Mechanisms of B-cell lymphoma pathogenesis. Nat Rev Cancer 2005; 5: 251–262.
22. Cattoretti G., Chang C.C., Cechova K., Zhang J., Ye B.H., Falini B., et al. BCL-6 protein is expressed in germinal-center B cells. Blood 1995; 86: 45–53.
23. Ye B.H., Cattoretti G., Shen Q., Zhang J., Hawe N., de Waard R., et al. The BCL-6 proto-oncogene controls germinal-centre formation and Th2-type inflammation. Nat Genet 1997; 16: 161–170.
24. Fearon D.T., Manders P.M., Wagner S.D. Bcl-6 uncouples B lymphocyte proliferation from differentiation. Adv Exp Med Biol 2002; 512: 21–28.
25. Fujita N., Jaye D.L., Kajita M., Geigerman C., Moreno C.S., Wade P.A. MTA3, a Mi-2/NuRD complex subunit, regulates an invasive growth pathway in breast cancer. Cell 2003; 113: 207–219.
26. Tunyaplin C., Shaffer A.L., Angelin-Duclos C.D., Yu X., Staudt L.M., Calame K.L. Direct repression of prdm1 by Bcl-6 inhibits plasmacytic differentiation. J Immunol 2004; 173: 1158–1165.
27. Saito M., Gao J., Basso K., Kitagawa Y., Smith P.M., Bhagat G., et al. A Signaling Pathway Mediating Downregulation of BCL6 in Germinal Center B Cells Is Blocked by BCL6 Gene Alterations in B Cell Lymphoma. 2007; 12: 280–292.
28. Ye B.H., Lista F., Lo Coco F., Knowles D.M., Offit K., Chaganti R.S., et al. Alterations of a zinc finger-encoding gene, BCL-6, in diffuse large-cell lymphoma. Science 1993; 262: 747–750.
29. Baron B.W., Anastasi J., Montag A., Huo D., Baron R.M., Karrison T., et al. The human BCL6 transgene promotes the development of lymphomas in the mouse. Proc Natl Acad Sci USA 2004; 101: 14198–14203.
30. Cattoretti G., Pasqualucci L., Ballon G., Tam W., Nandula S.V., Shen Q., et al. Deregulated BCL6 expression recapitulates the pathogenesis of human diffuse large B cell lymphomas in mice. Cancer Cell 2005; 7: 445–455.
31. Polo J.M., Dell'Oso T., Ranuncolo S.M., Cerchietti L., Beck D., Da Silva G.F., et al. Specific peptide interference reveals BCL6 transcriptional and oncogenic mechanisms in B-cell lymphoma cells. Nat Med 2004; 10: 1329–1335.
32. Cerchietti L.C., Yang S.N., Shaknovich R., Hatzi K., Polo J.M., Chadburn A., et al. A peptomimetic inhibitor of BCL6 with potent antilymphoma effects in vitro and in vivo. Blood 2009; 113: 3397–3405.
33. Chen L., Monti S., Juszczynski P., Daley J., Chen W., Witzig T.E., et al. SYK-dependent tonic B-cell receptor signaling is a rational treatment target in diffuse large B-cell lymphoma. Blood 2008; 111: 2230–2237.
34. Polo J.M., Juszczynski P., Monti S., Cerchietti L., Ye K., Greally J.M., et al. Transcriptional signature with differential expression of BCL6 target genes accurately identifies BCL6-dependent diffuse large B cell lymphomas. Proc Natl Acad Sci U S A 2007; 104: 3207–3212.
35. Braselmann S., Taylor V., Zhao H., Wang S., Sylvain C., Baluom M., et al. R406, an orally available spleen tyrosine kinase inhibitor

blocks fc receptor signaling and reduces immune complex-mediated inflammation. J Pharmacol Exp Ther 2006; 319: 998–1008.
36. Irish J.M., Czerwinski D.K., Nolan G.P., Levy R. Altered B-cell receptor signaling kinetics distinguish human follicular lymphoma B cells from tumor-infiltrating nonmalignant B cells. Blood 2006; 108: 3135–3142.
37. Phan R.T., Dalla-Favera R. The BCL6 proto-oncogene suppresses p53 expression in germinal-centre B cells. Nature 2004; 432: 635–639.
38. Fujita N., Jaye D.L., Geigerman C., Akyildiz A., Mooney M.R., Boss J.M., et al. MTA3 and the Mi-2/NuRD complex regulate cell fate during B lymphocyte differentiation. Cell 2004; 119: 75–86.
39. Niu H., Ye B.H., Dalla-Favera R. Antigen receptor signaling induces MAP kinase-mediated phosphorylation and degradation of the BCL-6 transcription factor. Genes Dev 1998; 12: 1953–1961.
40. Cornall R.J., Cheng A.M., Pawson T., Goodnow C.C. Role of Syk in B-cell development and antigen-receptor signaling. Proc Natl Acad Sci U S A 2000; 97: 1713–1718.
41. Shaffer A.L., Yu X., He Y., Boldrick J., Chan E.P., Staudt L.M. BCL-6 represses genes that function in lymphocyte differentiation, inflammation, and cell cycle control. Immunity 2000; 13: 199–212.
42. Dent A.L., Shaffer A.L., Yu X., Allman D., Staudt L.M. Control of inflammation, cytokine expression, and germinal center formation by BCL-6. Science 1997; 276: 589–592.
43. Oberley M.J., Tsao J., Yau P., Farnham P.J. High-throughput screening of chromatin immunoprecipitates using CpG-island microarrays. Methods Enzymol 2004; 376: 315–334.
44. Trinklein N.D., Aldred S.F., Hartman S.J., Schroeder D.I., Otillar R.P., Myers R.M. An abundance of bidirectional promoters in the human genome. Genome Res 2004; 14: 62–66.
45. Juszczynski P., Kutok J.L., Li C., Mitra J., Aguiar R.C., Shipp M.A. BAL1 and BBAP are regulated by a gamma interferon-responsive bidirectional promoter and are overexpressed in diffuse large B-cell lymphomas with a prominent inflammatory infiltrate. Mol Cell Biol 2006; 26: 5348–5359.
46. Castillo-Davis C.I., Hartl D.L. GeneMerge—post-genomic analysis, data mining, and hypothesis testing. Bioinformatics 2003; 19: 891–892.
47. Benjamini Y., Drai D., Elmer G., Kafkafi N., Golani I. Controlling the false discovery rate in behavior genetics research. Behav Brain Res 2001; 125: 279–284.
48. Reiner A., Yekutieli D., Benjamini Y. Identifying differentially expressed genes using false discovery rate controlling procedures. Bioinformatics 2003; 19: 368–375.
49. Subramanian A., Tamayo P., Mootha V.K., Mukherjee S., Ebert B.L., Gillette M.A., et al. Gene set enrichment analysis: a knowledge-based approach for interpreting genome-wide expression profiles. Proc Natl Acad Sci U S A 2005; 102: 15545–15550.
50. Aguiar R.C., Yakushijin Y., Kharbanda S., Tiwari S., Freeman G.J., Shipp M.A. PTPROt: an alternatively spliced and developmentally regulated B-lymphoid phosphatase that promotes G0/G1 arrest. Blood 1999; 94: 2403–2413.
51. Klein U., Tu Y., Stolovitzky G.A., Keller J.L., Haddad J., Jr., Miljkovic V., et al. Transcriptional analysis of the B cell germinal center reaction. Proc Natl Acad Sci U S A 2003; 100: 2639–2644.
52. Ranuncolo S.M., Polo J.M., Dierov J., Singer M., Kuo T., Greally J., et al. Bcl-6 mediates the germinal center B cell phenotype and lymphomagenesis through transcriptional repression of the DNA-damage sensor ATR. Nat Immunol 2007; 8: 705–714.
53. Irish J.M., Czerwinski D.K., Nolan G.P., Levy R. Kinetics of B cell receptor signaling in human B cell subsets mapped by phosphospecific flow cytometry. J Immunol 2006; 177: 1581––1589.
54. Chen L., Juszczynski P., Takeyama K., Aguiar R.C., Shipp M.A. Protein tyrosine phosphatase receptor-type O truncated (PTPROt) regulates SYK phosphorylation, proximal B-cell-receptor signaling, and cellular proliferation. Blood 2006; 108: 3428–3433.
55. Campbell K.S. Signal transduction from the B cell antigen-receptor. Curr Opin Immunol 1999; 11: 256–264.
56. Dal Porto J.M., Gauld S.B., Merrell K.T., Mills D., Pugh--Bernard A.E., Cambier J. B cell antigen receptor signaling 101. Mol Immunol 2004; 41: 599–613.
57. Johnson G.L., Lapadat R. Mitogen-activated protein kinase pathways mediated by ERK, JNK, and p38 protein kinases. Science 2002; 298: 1911–1912.
58. Amoui M., Baylink D.J., Tillman J.B., Lau K.H. Expression of a structurally unique osteoclastic protein-tyrosine phosphatase is driven by an alternative intronic, cell type-specific promoter. J Biol Chem 2003; 278: 44273–44280.
59. Friedberg J.W., Sharman J., Schaefer-Cutillo J., Johnston P.B., De Vos S., LaCasce A.L., J.P., et al. Fostamatinib Disodium (FosD), An Oral Inhibitor of Syk, Is Well-Tolerated and Has Significant Clinical Activity in Diffuse Large B Cell Lymphoma (DLBCL) and Chronic Lymphocytic Leukemia (SLL/CLL). Blood (ASH Annual Meeting Abstracts) 2008; 112: Abstract 3.
60. Seimiya H., Sawabe T., Inazawa J., Tsuruo T. Cloning, expression and chromosomal localization of a novel gene for protein tyrosine phosphatase (PTP-U2) induced by various differentiation-inducing agents. Oncogene 1995; 10: 1731–1738.
61. Wiggins R.C., Wiggins J.E., Goyal M., Wharram B.L., Thomas P.E. Molecular cloning of cDNAs encoding human GLEPP1, a membrane protein tyrosine phosphatase: characterization of the GLEPP1 protein distribution in human kidney and assignment of the GLEPP1 gene to human chromosome 12p12-p13. Genomics 1995; 27: 174–181.
62. Cheng A.M., Rowley B., Pao W., Hayday A., Bolen J.B., Pawson T. Syk tyrosine kinase required for mouse viability and B-cell development. Nature 1995; 378: 303–306.
63. Turner M., Gulbranson-Judge A., Quinn M.E., Walters A.E., MacLennan I.C., Tybulewicz V.L. Syk tyrosine kinase is required for the positive selection of immature B cells into the recirculating B cell pool. J Exp Med 1997; 186: 2013–2021.
64. Colucci F., Guy-Grand D., Wilson A., Turner M., Schweighoffer E., Tybulewicz V.L., et al. A new look at Syk in alpha beta and gamma delta T cell development using chimeric mice with a low competitive hematopoietic environment. J Immunol 2000; 164: 5140–5145.
65. Ci W., Polo J.M., Cerchietti L., Shaknovich R., Wang L., Yang S.N., et al. The BCL6 transcriptional program features repression of multiple oncogenes in primary B-cells and is deregulated in DLBCL. Blood 2009;blood-2008-12-193037 [Epub ahead of print].